Water Resources Research

RESEARCH ARTICLE
10.1029/2018WR022575

# Disaggregating Soil Moisture to Finer Spatial Resolutions: A Comparison of Alternatives

**Hoori Ajami**[1] and **Ashish Sharma**[2]

[1]Department of Environmental Sciences, University of California Riverside, Riverside, CA, USA, [2]School of Civil and Environmental Engineering, University of New South Wales, Sydney, New South Wales, Australia

**Key Points:**
- Application of four disaggregation alternatives to disaggregate catchment mean soil moisture to fine resolution is examined
- A univariate first-order autoregressive model is the best performing model to represent spatial heterogeneity and temporal persistence
- Only 10 days of fine-resolution hydrologic model simulations is required for parameterizing the disaggregation model

**Supporting Information:**
- Supporting Information S1

**Correspondence to:**
H. Ajami,
hooria@ucr.edu

**Citation:**
Ajami, H., & Sharma, A. (2018). Disaggregating soil moisture to finer spatial resolutions: A comparison of alternatives. *Water Resources Research*, *54*, 9456–9483. https://doi.org/10.1029/2018WR022575

Received 10 JAN 2018
Accepted 9 OCT 2018
Accepted article online 19 OCT 2018
Published online 27 NOV 2018



**Abstract** The spatial and temporal variability in soil moisture modulates runoff generation and the degree of land-atmosphere coupling. Numerous statistical and modeling approaches have been implemented to characterize soil moisture spatial heterogeneity at fine spatial resolution using data from sparse observational networks or distributed model simulations. This characterization has been subsequently employed to translate coarse model simulations (of the order of a few hundred meters or kilometers) to finer spatial scales for a range of ensuing applications that rely on high-resolution characterization of soil moisture. One common feature of these disaggregation methods is that the impact of soil moisture memory is ignored. This results in both spatial and temporal persistence being poorly simulated, leading to poorer specifications of cropping and irrigation plans. To overcome this shortcoming, we developed a hybrid disaggregation method that uses the first-order autoregressive model (AR1) constructed from fine-resolution (60 m) soil moisture simulations to disaggregate catchment mean soil moisture obtained from remote sensing or semidistributed model simulations. Soil moisture simulations from an integrated land surface-groundwater model, ParFlow-Common Land Model in Baldry subcatchment, Australia, are used as virtual observations. We examined the AR1 method performance against topographic wetness index-based methods and those developed from temporal stability method. Results illustrate that the disaggregation schemes calibrated to a 10-day fine-scale model simulation perform better than the topographic-based methods in approximating soil moisture distribution at a 60-m resolution in the catchment. Furthermore, the AR1 model is the best model (Nash-Sutcliffe efficiency [NSE] $>$ 0.45) among various alternatives explored here. Applying the hybrid univariate AR1 model is promising for disaggregating semidistributed models' soil moisture simulations while significantly reducing the computational time.

## 1. Introduction

Spatial and temporal variability of soil moisture modulates hydrologic and meteorological processes (Gaur & Mohanty, 2013) including water and energy balances partitioning at the land surface, runoff generation, and land-atmosphere coupling (Koster et al., 2000). Previous investigations have shown that soil moisture spatial variability is impacted by physical attributes of a landscape (topography, vegetation type, and soil properties) as well as dynamic attributes such as precipitation and potential evapotranspiration (Joshi et al., 2011; Reynolds, 1970). However, the degree of influence of these factors varies across catchments depending on the observations scale (local to regional; Seneviratne et al., 2010). As a result, it is almost impossible to separate the role of individual factors in describing soil moisture spatial patterns particularly from observations (Gaur & Mohanty, 2013). Overcoming the challenge at fine spatial resolutions (10 to 100 m) is important for a range of hydrological and water management applications and requires effective utilization of sparse field-scale soil moisture observational networks and coarse-resolution remotely sensed soil moisture products (Vereecken et al., 2012).

Hyperresolution distributed hydrologic models provide a quantitative framework for characterizing dynamics of soil moisture spatial variability (Fatichi et al., 2016; Wood et al., 2011). However, regional scale implementation of integrated hydrologic models at fine spatial resolution is computationally intensive. One approach to reduce computational demand of distributed hydrologic models is to upscale fine-resolution parameter sets to coarse resolution (of the order of a few hundred meters) and derive model simulations at the coarse spatial resolution scale. For example, Jana and Mohanty (2012b) showed that the power-averaging algorithm can provide reasonable estimate of effective soil hydraulic parameters at coarse scale. This upscaling procedure can represent fine-scale soil moisture heterogeneity at large scale while

reducing bias (Jana & Mohanty, 2012a). Alternatively, application of semidistributed hydrologic models reduces computational time by performing simulations on representative parts of a landscape defined as Hydrologic Response Units (HRUs). Either way, representing fine-scale spatial heterogeneity of soil moisture dynamics is a problem that still remains, whether one uses semidistributed or coarse-resolution distributed models to simulate land surface fluxes across the landscape.

Table 1 provides an overview of existing approaches to characterize and represent fine-scale soil moisture spatial heterogeneity. In general, these methods are classified to three groups (Pau et al., 2016): (I) statistical methods based on soil moisture observations to establish statistical relationships between spatial mean soil moisture and its higher-order attributes such as standard deviation and the coefficient of variation, (II) modeling approaches that implicitly infer fine-scale soil moisture distributions from hydrologic or land surface models simulations, and (III) disaggregation methods for downscaling remotely sensed soil moisture products using fine-resolution vegetation (Kim et al., 2017), optical or thermal satellite products (Merlin et al., 2008, 2013), or fine-resolution hydrologic or land surface models (Pau et al., 2016).

A review of statistical relationships between the soil moisture spatial mean and its standard deviation across various sites reveals a range of relationships from linear functions to convex relationships with peak values at intermediate soil moisture content and with many sites exhibiting no systematic trend (Korres et al., 2015). As a result, no universal relationship has been identified between the soil moisture spatial mean and its higher order statistics, and parameters of these functions are often specified depending on the topography, soil, and vegetation types of a site. Kim et al. (2016) showed that in zero-order catchments soil moisture spatial patterns are different for the same spatial mean soil moisture. The nonuniqueness of soil moisture spatial patterns depends on, among others, the drainage condition, and the degree of coupling between surface soil moisture and water content at deeper depths as well as seasonality (Rosenbaum et al., 2012).

Topography is often assumed as a key contributor to soil moisture spatial variability. Availability of digital elevation models and advancements in geographic information systems have led to development of terrain-based indices for disaggregating catchment-scale soil moisture estimates or interpolating sparse soil moisture observations. However, these approaches are often implemented without investigating whether topography is the main factor controlling soil moisture spatial patterns (Grayson & Western, 2001). Western et al. (2004) showed that at some sites variability of soil properties plays a more important role than the topography. Pellenq et al. (2003) also illustrated that the combined topographic wetness index (TWI; ratio of upslope contributing area per unit contour to local slope angle; Beven & Kirkby, 1979) and soil depth information compared to topography alone improves catchment-scale soil moisture disaggregation in a low relief catchment (Pellenq et al., 2003). Later, Wilson et al. (2005) developed a multiple linear regression model for predicting soil moisture spatial patterns as a function of digital elevation model-derived attributes and catchment-averaged soil moisture. Therefore, their approach relies on spatially distributed observations for a range of average soil moisture conditions that may not be available in all cases (Wilson et al., 2005).

Model-based soil moisture disaggregation approaches range from simple mapping of soil moisture fields from simulations performed at similar HRUs (Chaney et al., 2016), application of terrain-based indices such as TWI (Beven & Kirkby, 1979) for soil moisture distribution (Koster et al., 2000; Pellenq et al., 2003), establishing statistical relationships between the coarse- and fine-resolution simulations using advanced statistical methods (Pau et al., 2016), to changes in constitutive model equations for incorporating subgrid variability (Choi et al., 2007). Table 1 provides further details about the methodology, advantages, and disadvantages of each approach. Satellite remote sensing soil moisture products such as microwave products provide information about soil moisture distribution at regional and global scales. However, their application at catchment scale is limited by their coarse spatial resolution and lower penetration depth (Mohanty et al., 2017). Downscaling of remotely sensed soil moisture products can provide information about soil moisture spatial variability at fine scale. In recent years, variety of methods have developed based on (I) fine-resolution optical or thermal remote sensing products (Merlin et al., 2008, 2013), (II) developing statistical relationships between fine-resolution hydrologic or land surface model simulations and coarse-resolution satellite soil moisture (Loew & Mauser, 2008), and (III) deterministic downscaling approaches based on remote sensing soil moisture and/or evapotranspiration products for soil hydraulic parameter estimation in fine-resolution hydrologic models (Shin & Mohanty, 2013). A recent review of downscaling approaches for remote sensing soil moisture products is provided by Peng et al. (2017).

**Table 1**
*Summary of Various Soil Moisture Disaggregation Approaches*

| Approach | Main inputs | Outcome/benefits | Limitations | Source |
|---|---|---|---|---|
| Statistical methods based on soil moisture observations | | | | |
| Presenting soil moisture scaling properties as a function of aggregation scale | ESTAR[a] data | Soil moisture spatial variance decreases with increasing the averaging area | Developing these empirical relationships requires lots of data | Rodriguez-Iturbe et al. (1995) |
| Exploring the relationships between the spatial mean soil moisture and its higher-order statistics | Soil moisture in-situ probes | Soil moisture spatial standard deviation is decreasing with increases in moisture conditions | Developing these relationships requires lots of data | Famiglietti et al. (1999) |
| Modeling approaches that implicitly represent fine-scale soil moisture patterns | | | | |
| Direct mapping of simulated soil moisture for each HRU to similar HRUs in the domain | Semidistributed hydrologic modeling | Reducing computational time | Accuracy of spatial patterns depends on the assumptions and data used to delineate HRUs | Ajami et al. (2016) and Chaney et al. (2016) |
| Transforming catchment scale water table distribution to root zone soil moisture distribution based on the TWI distribution | TWI is indirectly used to distribute catchment mean soil moisture | Reducing computational time | Accuracy of soil moisture spatial patterns depends on water table distributions and assuming equilibrium soil moisture distribution above the water table | Koster et al. (2000) |
| Disaggregating catchment mean soil moisture from a model to fine resolution using topography and soil depth data | Model based | Spatially distributed soil moisture patterns particularly in relatively wet states are obtained by using topography and soil depth data | Performance depends on the scale and catchment characteristics | Pellenq et al. (2003) |
| Formulating multiple linear regression models to predict point-scale soil moisture from the spatial mean soil moisture and spatial distribution of topographic attributes | Field-based observations | Accounts for changes in spatial mean soil moisture to characterize fine-scale soil moisture spatial distributions | Needs large datasets with good spatial coverage to establish the relationships while considering a range of moisture conditions | Wilson et al. (2005) |
| Deriving the volume-averaged Richards equation to account for subgrid topographic variability | Model based | Incorporating sub-grid scale soil moisture variability into the governing equations derived for coarse-resolution simulations | Topography is the main driver of soil moisture variability in a grid cell and soil properties are constant in a large grid cell | Choi et al. (2007) |
| Establishing the relationships between spatial mean soil moisture and its higher order statistics using fine-scale simulations and predicting its higher moments from coarse-resolution simulations | Model based (PAWS[b]-CLM4) | A computationally efficient approach for obtaining higher-order moments of soil moisture distribution from the mean obtained from coarse-resolution simulations | The surrogate models only predict higher-order moments at coarse scale, and they do not map back the mean soil moisture to finer resolutions | Riley and Shen (2014) |
| Applying the proper orthogonal decomposition mapping method to establish spatially explicit relationships between the fine- and coarse-resolution model simulations | Model based (PAWS-CLM) | A computationally efficient approach for obtaining fine-scale soil moisture and land surface fluxes distributions from coarse-resolution models | Reduced-order models are site specific and their development is computationally intensive | Pau et al. (2016) |
| Developing autoregressive models from fine-scale model simulations to disaggregate | Model based (ParFlow-CLM) | A computationally efficient approach to obtain fine-scale soil moisture distributions from | Relies on fine-resolution model simulations | This study |

**Table 1** *(continued)*

| Approach | Main inputs | Outcome/benefits | Limitations | Source |
|---|---|---|---|---|
| spatial mean soil moisture from coarse-resolution or semidistributed simulations | | coarse-resolution models while considering soil moisture memory effect | | |
| Disaggregation methods based on remotely sensed data | | | | |
| Downscaling of satellite soil moisture using finer-resolution satellite data and disaggregation algorithms like DISPATCH[c] | Downscaling of SMOS[d] soil moisture observations based on satellite-derived evaporative efficiency data at 1 km | Using available fine-resolution satellite products for downscaling | Only provides soil moisture for the top few centimeters of the soil profile | Merlin et al. (2008, 2013) |
| Disaggregating remotely sensed soil moisture products by using fine-resolution land surface model simulations to establish linear regressions between the spatial mean soil moisture and fine-scale simulations | Model based | Relatively good performance | Disaggregated soil moisture values are sensitive to bias in satellite soil moisture retrievals | Loew and Mauser (2008) |
| Deterministic downscaling of remotely sensed soil moisture data using a fine-resolution hydrologic model calibrated to remotely sensed soil moisture and evapotranspiration | Soil hydraulic parameters are constrained in a way that mean soil moisture and evapotranspiration from the simulated domain match the remote sensing products | It is only tested for limited conditions and the optimization approach is computationally intensive for large domains | Quality of disaggregated soil moisture depends on the quality of remote sensing data | Shin and Mohanty (2013) |

*Note*. TWI = topographic wetness index; HRU = Hydrologic Response Unit; CLM = Common Land Model.
[a]ESTAR = Electronically steered thinned array radiometer. [b]PAWS = Process-based Adaptive Watershed Simulator. [c]DISPATCH = Disaggregation based on physical and theoretical scale change. [d]SMOS = Soil moisture and ocean salinity.

While various approaches are developed to overcome the disconnection between in situ soil moisture measurements and satellite products (Jawson & Niemann, 2007), application of each method has certain limitations as outlined in Table 1. These include reliance on dense observational network, intensive computational demands, difficulty in identifying the dominant factors controlling soil moisture spatial variability (Gaur & Mohanty, 2013), and nonuniqueness of empirical equations. One of the main characteristics of the above disaggregation methods is that the role of soil moisture memory is often ignored with the exception of deterministic downscaling methods (Shin & Mohanty, 2013). This means that a disaggregation method is applied independently of soil moisture content from the previous time step.

To overcome this shortcoming, we developed a hybrid statistical approach based on a first-order autoregressive (AR1) model to disaggregate coarse scale, hillslope, or catchment-averaged soil moisture, using information from a dense observational network or high-resolution (of the order of 10- to 100-m resolution) model simulations. The benefit of the AR1 model, compared to other statistical approaches, is on incorporating the soil moisture memory effect on spatial disaggregation of mean catchment soil moisture while assuming that the soil moisture spatial mean is a priori known. To our knowledge, this is the first time that autoregressive methods have been implemented for soil moisture disaggregation. To enhance the quality of the disaggregated output, we address three key questions: (I) Does topography exert a first-order control on soil moisture spatial distribution at catchment scale? (II) How to approximate soil moisture spatial variability using information content of fine-resolution soil moisture simulations? and (III) Which disaggregation alternative best describes soil moisture spatial variability in a range of conditions using multiple model performance measures?

As fine-scale spatially distributed soil moisture observations at catchment scale are seldom available, soil moisture simulations from an integrated land surface-groundwater model, ParFlow-Common Land Model (CLM), (Kollet & Maxwell, 2008) are used as the basis to examine the performance of alternate disaggregation methods. These methods are based on the TWI (Beven & Kirkby, 1979), temporal stability analysis (Vachaud et al., 1985), and different formulations of autoregressive models, as described later.

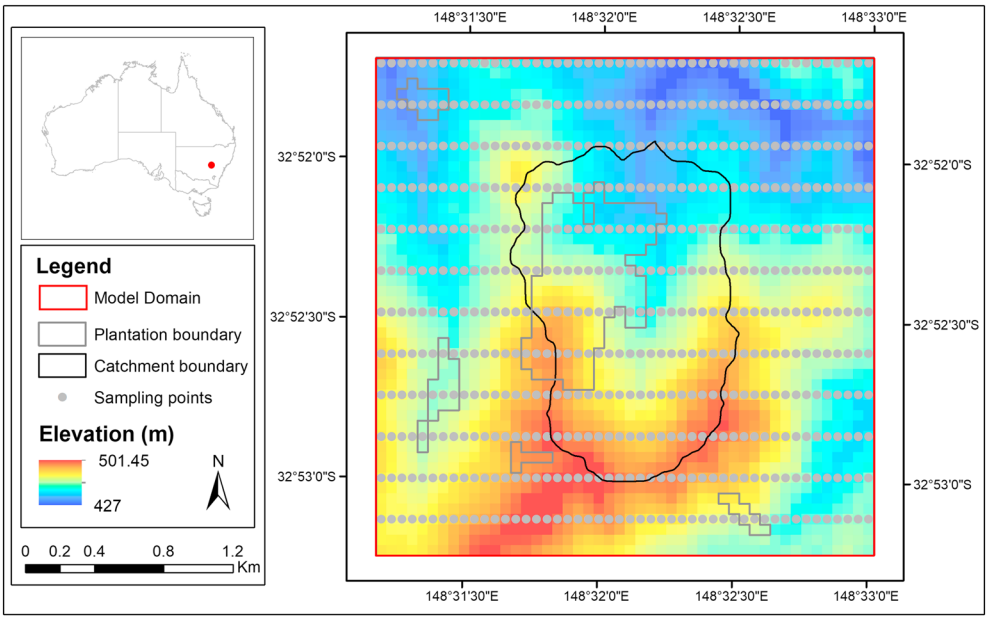


**Figure 1.** Baldry catchment in central New South Wales, Australia. Lower elevation regions are shown in dark blue. The sampling points show pixels of cross-section locations for soil moisture disaggregation methods based on distributed cross-section model simulations or limited sampling data (section 4.1.1).

## 2. Materials and Methods

### 2.1. Study Area

The Baldry subcatchment in central western New South Wales, Australia, has an area of 1.9 $km^2$ (Figure 1). Grasslands cover 72% of the catchment area, and the remainder is covered by eucalyptus plantation forest. This ephemeral catchment has a mild topography with elevation ranges from 443 to 500 m. According to the Koppen-Geiger classification, climate is temperate with hot summers (Peel et al., 2007). Meteorological observations from the weather station at the site indicate mean annual precipitation of 741.3 ± 292 mm during 2004–2010 period. One of the notable features of this period is occurrence of a dry (2006) and wetter than average (2010) year with annual precipitations of 278 and 1,279 mm, respectively.

### 2.2. ParFlow-CLM Framework

The integrated hydrologic model code ParFlow-CLM (Ashby & Falgout, 1996; Jones & Woodward, 2001; Kollet & Maxwell, 2006) is implemented for the Baldry catchment to simulate variably saturated subsurface flow using the Richards equation (Richards, 1931). ParFlow overland flow simulator routes ponded water on the land surface using the kinematic wave equation (Kollet & Maxwell, 2006). The CLM 3.0 (Dai et al., 2003) is modified and integrated into ParFlow for simulating water and energy fluxes at the land surface (Kollet & Maxwell, 2008; Maxwell & Miller, 2005). All the energy balance components (net radiation, sensible and latent heat fluxes, and ground heat flux) in CLM are dependent on calculated soil moisture from ParFlow. Latent heat flux is the sum of ground evaporation, evaporation from wet foliage, and plant transpiration in which their magnitudes are dependent on air specific humidity, aerodynamic and stomatal resistances, conductance of heat and vapor fluxes from leaves, wetted area, potential evaporation, and leaf area index (Kollet & Maxwell, 2008).

The ParFlow-CLM model domain for the Baldry sub-catchment was set up over a 2.9 km by 2.9 km area encompassing the catchment (Figure 1). Horizontal resolution of the modeling grid is 60 × 60 m, and the vertical discretization is 0.5 m. This configuration results in 48 × 48 × 203 grid cells. As the bottom elevation of the domain is set to a uniform 400 m elevation, the subsurface thickness becomes variable with thicknesses ranging from 43 to 101 m across the domain. Boundary conditions of a computational domain include ParFlow free-surface overland flow boundary condition at the land surface (Manning's roughness coefficient of 5.52E-6 [$hr/m^{1/3}$]) and a no-flow boundary condition for the bottom and lateral boundaries. Prescribed subsurface hydraulic parameters are as follows: saturated hydraulic conductivity (0.18 [m/h]),

van Genuchten parameters (1.5 [1/m] and $n = 2$), relative residual saturation (0.1) where relative saturation is the ratio of volumetric water content to porosity, and porosity (0.25; Acworth & Brain, 2008).

The hourly spatially uniform forcing data for the 2004–2010 period are obtained from a weather station at the site. Hourly downward longwave radiation data are from the Modern Era Retrospective Analysis for Research and Applications reanalysis data interpolated to 0.25° × 0.25° resolution (Decker et al., 2012). For model initialization, the hybrid spin-up approach of Ajami et al. (2014) is implemented using 2004 forcing data until dynamic equilibrium is reached (Ajami et al., 2014). Dynamic equilibrium is specified when changes in monthly groundwater storage values during recursive simulations reached below 0.1%. Transient simulations cover 2005 to 2010 and are initialized using pressure head and land surface temperature distributions from the last day of spin-up simulations.

### 2.3. Spatial Disaggregation Methods

ParFlow-CLM daily soil moisture simulations from 2006, 2008, and 2010 are used for development and evaluation of spatial disaggregation methods as dense in situ observations are not available for this site. These simulations cover a range of wetness conditions in the catchment that characterize years with annual precipitation lower or higher than average. Total annual precipitation for 2006, 2008, and 2010 are 278 (dry), 780 (average), and 1,279 mm (wet), respectively.

We implemented four methods to disaggregate spatial mean catchment soil moisture to fine resolution (60 m). The 60-m spatial resolution corresponds to horizontal discretization of ParFlow-CLM for Baldry catchment. The disaggregation methods are based on (I) terrain derived indices, (II) temporal stability analysis, (III) univariate, and (IV) multivariate autoregressive models. While the first two methods have been used previously, this is the first time that autoregressive models are implemented for soil moisture disaggregation. Both temporal stability and autoregressive models assume that soil moisture temporal dynamics in neighboring locations are related despite the variability of absolute soil moisture values, consistent with Seneviratne et al. (2010). All these methods rely on availability of observed or simulated spatial mean soil moisture for every time step. This information can be obtained from remotely sensed soil moisture observations (e.g., Soil Moisture Active Passive) or computationally efficient semidistributed hydrologic modeling alternatives. For large catchments, subbasin-averaged soil moisture values can be used to disaggregate soil moisture in individual subbasins.

Details for each of the disaggregation models evaluated are presented in the following subsections. In the equations presented in this paper, bold characters stand for a vector or matrix and nonbold characters refer to a single value variable.

#### 2.3.1. Terrain-Based Indices

To address the question how topography controls soil moisture spatial distribution in the catchment, relationships between land surface elevation and TWI (Beven & Kirkby, 1979) and soil moisture distributions from ParFlow-CLM are explored. TWI distribution is implemented in TOPMODEL (a TOPography-based hydrological MODEL) for producing spatially distributed soil moisture and water table patterns (Quinn et al., 1995), and it has been widely used for spatial disaggregation of catchment mean soil moisture elsewhere. To disaggregate catchment-averaged soil moisture to spatially distributed soil moisture at every grid cell, the ratio of local TWI to catchment average TWI is calculated. This ratio, referred to as *relative wetness index*, is used to estimate the soil moisture as follows:

$$SM_{i,j}(\mathrm{t}) = \frac{TWI_{i,j}}{\overline{TWI}_{i,j}} \times \overline{SM}(t) \tag{1}$$

where $SM_{i,j}(t)$ is soil moisture at pixel $i,j$ at time $t$, $TWI_{i,j}$ is topographic wetness index value of pixel $i,j$, and $\overline{SM}(t)$ and $\overline{TWI}$ are catchment-averaged soil moisture at time $t$ and TWI, respectively. For large catchments, mean soil moisture from every subbasin can be used for disaggregation. In the case of remotely sensed observations such as Soil Moisture Active Passive with a spatial resolution of 9 km (Chan et al., 2018), soil moisture observation from every grid cell can represent mean soil moisture in equation (1). The only condition that equation (1) results in higher soil moisture values than the porosity is when the domain-averaged soil moisture is equal to the porosity, and all the pixels in the domain become saturated. While this condition did not happen in the catchment, even during the wettest year (2010), the algorithm checks for this condition and sets the soil moisture of every pixel to saturated water content.

#### 2.3.2. Temporal Stability Method

The concept of soil moisture temporal stability was first introduced by Vachaud et al. (1985) who found that soil moisture values from certain locations in the field are representative of mean field soil moisture. This concept was later expanded to find representative locations at watershed and regional scales for soil moisture monitoring (Vanderlinden et al., 2012). Loew and Mauser (2008) used this concept to disaggregate coarse-scale passive microwave soil moisture observations to fine resolution. They developed series of linear regression equations that relate time series of fine-resolution soil moisture simulations from a land surface model to spatially averaged soil moisture at coarse resolution. At every location, a linear regression equation has the form

$$SM_{i,j}(\mathrm{t}) = a_{i,j} + b_{i,j}\overline{SM}(t) \tag{2}$$

where $SM_{i,j}(t)$ is soil moisture at pixel $i,j$ at time $t$, $a_{i,j}$ and $b_{i,j}$ are the intercept and slope at pixel $i,j$, respectively, and $\overline{SM}(t)$ is spatially averaged soil moisture at time $t$. Loew and Mauser (2008) estimated regression coefficients from a 10-year soil moisture climatology simulated by the PROcess-oriented Multiscale EvapoTranspiration (PROMET) model (Mauser & Schädlich, 1998). The main assumptions of the temporal stability method are as follows: (I) coarse-scale soil moisture values (subbasin mean) are unbiased (Loew & Mauser, 2008) and (II) regression coefficients are time invariant (Perry & Niemann, 2007).

Here we used 10 days of soil moisture simulations from 1 to 10 January 2008 of ParFlow-CLM to estimate regression coefficients for every grid cell of the domain (Figure 1). The linear regression equations will predict fine-scale soil moisture values for the remaining days of 2008, 2006, and 2010 using catchment-averaged daily mean soil moisture from ParFlow-CLM. Later, disaggregation approach sensitivity to the length of calibration data is examined.

#### 2.3.3. Univariate AR1 Model

Autoregressive (AR) models have been widely used in hydrologic time series analysis for forecasting a variable of interest based on its values from previous time steps (Salas et al., 1980). AR models can have constant or time variant parameters and are classified as univariate or multivariate depending on the number of variables the time series represents. In the multivariate case, an AR model preserves temporal and spatial dependence across multiple variables (Westra et al., 2007). The main assumption of AR models is that the time series is stationary, and residuals are independent and identically distributed (Salas et al., 1980). Therefore, the AR models preserve the historical mean, correlation structure, and standard deviation of the time series when generating new replicates of the data.

Here we developed an approach assuming an AR1 to disaggregate catchment-scale mean soil moisture. An AR1 model has only one autoregressive term, or the soil moisture at location $i,j$ and time $t$ is only a function of the soil moisture value at the previous time step ($t-1$). As a result, the model is able to simulate persistence at the pixel scale, which is not the case with the temporal stability approach discussed earlier. The univariate first-order autoregressive model (UAR1) parameters are estimated using ParFlow-CLM soil moisture simulations from 1 to 10 January 2008. A UAR1 model has the following form:

$$Z_{i,j}(t) = A\,Z_{i,j}(t-1) + \varepsilon_t \tag{3}$$

where $Z_{i,j}(t)$ is the standardized soil moisture time series at pixel $i,j$ and time $t$, $A$ is the lag-1 autocorrelation, $Z_{i,j}(t-1)$ is the standardized time series at time $(t-1)$ at pixel $i,j$, and $\varepsilon_t$ is the error which is uncorrelated in time with zero mean (Salas et al., 1985). In the description below, the AR1 model formulations in equation (3) is adapted to (I) maintain aggregation across space to the mean soil moisture being disaggregated and (II) simulate persistence in time at each pixel based on location specific parameters. The steps involved are as follows:

1. Obtain fine-scale soil moisture simulations for an area of interest from ParFlow-CLM or any distributed hydrologic or land surface model at the spatial resolution of interest. The length of a time series can be as short as 10 days. A 10-day time series may be obtain from a single year of soil moisture observations or simulations or daily soil moisture climatology calculated from long-term averaging of daily simulations or observations (e.g., January 1st to 10th of years 2005–2010). We explore the role of time series length on deriving AR1 model parameters in the sensitivity analysis section.
2. For every time step, compute ratio of simulated soil moisture at a given pixel to subbasin or catchment-averaged soil moisture at that time step:

$$r_{i,j}(t) = \frac{SM_{i,j}(t)}{\overline{SM}(t)} \tag{4}$$

where $r_{i,j}(t)$ is the soil moisture ratio at pixel $i,j$ and time $t$, $SM_{i,j}(t)$ is soil moisture at pixel $i,j$ at time $t$, and $\overline{SM}(t)$ is spatially averaged soil moisture at time $t$. For large catchments, spatially averaged soil moisture is obtained for every subbasin. In the results presented later, the length of the ratio time series used to ascertain model parameters is equal to 10 days for each pixel.

3. Compute the $m$-day mean ratio at every pixel and standardize the sseries by subtracting the temporal mean (10-day average) at every time step

$$\begin{aligned} Z_{i,j}(t) &= r_{i,j}(t) - \widehat{\mu}_{i,j} \ \text{, and} \\ \widehat{\mu}_{i,j} &= \frac{\sum_{t=1}^{m} r_{i,j}(t)}{m} \end{aligned} \tag{5}$$

Here $Z_{i,j}(t)$ represents the standardized ratio at pixel $i,j$ and time $t$, $r_{i,j}(t)$ is the soil moisture ratio at pixel $i,j$ at time $t$, $\widehat{\mu}_{i,j}$ is the $m$-day mean soil moisture ratio at pixel $i,j$, and $m$ is the time series length (10 days).

4. Compute the lag-1 autocorrelation ($A$) using the standardized soil moisture ratio ($Z_{i,j}(t)$) at every pixel. The number of lag-1 autocorrelation values is equal to the total number of pixels in the domain (2,304 pixels in the Baldry catchment).
5. Use the lag-1 autocorrelation ($A$) and initial soil moisture value from the previous time step to estimate the standardized soil moisture ratio at pixel $i,j$ and time $t$ using

$$Z_{i,j}(t) = A\, Z_{i,j}(t-1) \tag{6}$$

where $Z_{i,j}(t)$ and $A$ are already described in equation (1), and $Z_{i,j}(t-1)$ is the standardized soil moisture ratio at time $(t-1)$ at pixel $i,j$. The error term $\varepsilon_t$ of equation (3) is ignored here and accounted for in the rescaling process in step 7.

6. Unstandardize $Z_{i,j}(t)$ to the soil moisture ratio as follows:

$$\widehat{r}_{i,j}(t) = Z_{i,j}(t) + \widehat{\mu}_{i,j} \tag{7}$$

where $\widehat{r}_{i,j}(t)$ is the predicted soil moisture ratio at pixel $i,j$ at time $t$, $Z_{i,j}(t)$ is the standardized soil moisture ratio at pixel $i,j$ and time $t$, and $\widehat{\mu}_{i,j}$ is the $m$-day mean soil moisture ratio at location $i,j$.

7. To preserve the catchment-scale mean soil moisture for the current time step, rescale the predicted ratio by the catchment or subbasin-averaged soil moisture obtained from coarse-resolution soil moisture simulations or remotely sensed data, $\overline{SM}(t)$.

$$\widehat{SM'}_{i,j}(t) = \widehat{r}_{i,j}(t) \times \frac{\overline{SM}(t)}{\overline{r}(t)} \tag{8}$$

where $\widehat{SM'}_{i,j}(t)$ is the predicted (disaggregated) soil moisture at pixel $i,j$ at time $t$, other notations remaining the same. This ratio adjusts the predicted time series mean to the subbasin mean while at the same time adjusting the spatial standard deviation by $\frac{\overline{SM}(t)}{\overline{r}(t)}$. Note that the mean of ratios is always equal to 1.

This rescaling approach adjusts the spatial variability of soil moisture without explicitly considering the relationship between catchment-averaged soil moisture and its standard deviation. However, it has been shown by Famiglietti et al. (2008) that spatial standard deviation varies as a function of mean soil moisture and extent. At small scales (less than 100 m), the relationship between standard deviation and mean soil moisture is convex upward while at larger extent becomes concave downward (Famiglietti et al., 2008). To rescale the mean and standard deviation of predicted soil moisture values, an empirical relationship between the subbasin level spatial standard deviation and mean soil moisture is developed using the ($m$ = 10)-day ParFlow-CLM simulations of 2008

$$\sigma_{\overline{SM}_{(t)}} = a + b\,\overline{SM}(t) \tag{9}$$

where $\sigma_{\overline{SM}_{(t)}}$ is the predicted spatial standard deviation at time $t$ based on spatial mean soil moisture $\overline{SM}(t)$, and $a$ and $b$ are empirical parameters estimated from a $m$-day calibration data. This empirical relationship predicts standard deviation at every time step using the subbasin-averaged soil moisture. The empirical function can have any form and is assumed linear as it best represents ParFlow-CLM simulation of the Baldry catchment.

The final rescaling equation based on the spatial mean and estimated standard deviation at time step t is

$$\widehat{SM}_{i,j}(t) = \overline{SM}(t) + \left[\widehat{SM'}_{i,j}(t) - \overline{SM}(t)\right]\frac{\sigma_{\overline{SM}_{(t)}}}{\sigma_{\widehat{SM}_{(t)}}} \tag{10}$$

where $\widehat{SM}_{i,j}(t)$ is the predicted (disaggregated) soil moisture at pixel $i,j$ at time $t$, $\sigma_{\overline{SM}_{(t)}}$ is predicted standard deviation from equation (9), and $\sigma_{\widehat{SM}_{(t)}}$ is the spatial standard deviation of estimated soil moisture $(\widehat{SM'}_{i,j}(t))$ in (8) over the domain. It should be noted that if a negative soil moisture value results from the estimation in (10), it is truncated to residual water content. However, in the simulation results presented later, such negative occurrences did not occur.

8. To predict soil moisture for the next time step using equation (6), the estimated $\widehat{SM}_{i,j}(t)$ from equation (10) is first standardized using equations (4) and (5) and the process will continue for additional time steps.

#### 2.3.4. Multivariate AR1 Model

Multivariate AR1 models consider time dependence as well as cross correlations of multiple time series. This implies that soil moisture predictions at location $i,j$ and time $t$ are a function of previous day soil moisture and cross correlations of the soil moisture time series at this pixel with other pixels in the domain. A multivariate AR1 model has the form

$$\boldsymbol{Z_{i,j}}(\mathrm{t}) = \mathbf{A}\boldsymbol{Z_{i,j}}(\mathrm{t}-1) + \mathbf{B}\,\boldsymbol{\varepsilon_t} \tag{11}$$

where $\boldsymbol{Z_{i,j}(t)}$ is the standardized time series at pixel $i,j$ and time $t$, $\mathbf{A}$ and $\mathbf{B}$ are $n \times n$ parameter matrices, and $\varepsilon_t$ represents the independent and identically distributed noise vector with zero mean and unit standard deviation (Salas et al., 1980). Similar to the univariate AR1 model, soil moisture time series data from fine-scale simulations are standardized using the procedure outlined in steps 1 to 3. The difference here is in computing model parameters where $\mathbf{A}$ is now a $(n \times n)$ matrix with $n$ equal to the number of pixels in the domain. The method of moments estimate of the parameters in $\mathbf{A}$ is written as (Matalas, 1967)

$$\widehat{\mathbf{A}} = \widehat{\boldsymbol{M}}_{\mathbf{1}}\,\widehat{\boldsymbol{M}}_{\mathbf{0}}^{-\mathbf{1}} \tag{12}$$

where $\widehat{\boldsymbol{M}}_{\mathbf{0}}$ and $\widehat{\boldsymbol{M}}_{\mathbf{1}}$ are the lag-0 and lag-1 cross-correlation matrices. The elements of $\boldsymbol{M}_{\mathbf{0}}$ and $\boldsymbol{M}_{\mathbf{1}}$ matrices are lag-0 and lag-1 auto and cross correlations values computed from the standardized soil moisture time series. A general form of matrix $\boldsymbol{M}$ for a domain with size $n$ is

$$\widehat{\boldsymbol{M}_{\boldsymbol{k}}} = \begin{bmatrix} \rho_k^{11}, \rho_k^{12}, & \cdots, & \rho_k^{1n} \\ \vdots & \ldots & \vdots \\ \rho_k^{n1}, \rho_k^{n2}, & \cdots & \rho_k^{nn} \end{bmatrix} \tag{13}$$

where $\rho_k^{ij}$ is the lag-k cross-correlation coefficient between $Z_i(t)$ and $Z_j(t-1)$ for $i \neq j$. If $i = j$, then $\rho_k^{ij}$ is the autocorrelation coefficient of order $k$. Once matrix $\mathbf{A}$ is calculated, soil moisture predictions and scaling is similar to steps 5 to 7 of the univariate AR1 model. Due to the soil moisture rescaling in step 7, the second term on the right-hand side of equation (11) is eliminated.

It is evident from equations (12) and (13) that a multivariate AR1 model has a large number of parameters to account for time and cross dependence between multiple time series. This complexity may result in large estimation errors if the number of observations for parameter estimation are limited. Therefore, it is possible to simplify the model structure to reduce the number of parameters. One simple approximation is to diagonalize the $\mathbf{A}$ matrix by setting the off diagonal elements to zero (Mehrotra & Sharma, 2015; Salas et al., 1985).

This means that the lag-1 cross correlations are not important in soil moisture predictions. Indeed, our initial investigations showed that using the full **A** matrix introduces large errors in predicted initial soil moisture values at the first few time steps. However, the error will dissipate with time. As a result, only the diagonal elements of the **A** matrix are used to create a contemporaneous multivariate AR1 model referred to as MAR1 in the remainder of this paper.

### 2.4. Model Evaluation Measures

Two types of model evaluation measures are used to compare disaggregated soil moisture with soil moisture simulations from ParFlow-CLM at every time step. These measures are (1) root-mean-square difference (RMSD), Nash-Sutcliffe efficiency (NSE) and Kling-Gupta efficiency (KGE; Gupta et al., 2009) for cell-to-cell comparison and (2) an empirical orthogonal function (EOF) analysis for comparing spatial patterns of disaggregated and simulated soil moisture (Koch et al., 2015). An additional evaluation metrics is implemented to compare pixel-scale temporal dependence of disaggregated soil moisture with ParFlow-CLM simulations.

#### 2.4.1. Cell-to-Cell Evaluation

The following metrics were computed between estimated fine-scale soil moisture from a disaggregation approach and ParFlow-CLM simulation at every time step. These represent aggregated measures of a disaggregation method performance over a spatial domain of interest.

$$RMSD = \sqrt{\frac{1}{N}\sum_{i=1}^{N}(B_i - M_i)^2} \tag{14}$$

$$NSE = 1 - \frac{\sum_{i=1}^{N}(B_i - M_i)^2}{\sum_{i=1}^{N}\left(B_i - \overline{B}\right)^2} \tag{15}$$

$$KGE = 1 - \sqrt{(r-1)^2 + (\alpha - 1)^2 + (\beta - 1)^2}, \alpha = \frac{\sigma_M}{\sigma_B}, \beta = \frac{\mu_M}{\mu_B}, \tag{16}$$

where $N$ is total number of pixels in a domain, $B_i$ is the ParFlow-CLM simulated soil moisture for pixel $i$, $M_i$ is the estimated soil moisture from a disaggregation method at pixel $i$, $r$ is the linear correlation coefficient between ParFlow-CLM soil moisture simulations and a disaggregation method, $\alpha$ is a measure of relative variability and is the ratio of spatial standard deviations of a disaggregated soil moisture over the domain ($\sigma_M$) to ParFlow-CLM simulations ($\sigma_B$), and $\beta$ represents bias and is the ratio between the soil moisture spatial mean ($\mu$) from a disaggregation method ($\mu_M$) and ParFlow-CLM ($\mu_B$) for every time step. Due to the rescaling in step 7, $\beta$ is equal to 1. The value of RMSD depends on the unit of a variable and ranges between 0 and $\infty$. The range of NSE values is between 1 and $-\infty$ where 1 indicates a perfect fit and values less than zero indicate that the observation's mean is a better predictor than the model simulation. KGE of 1 represents a perfect fit and it is more informative than the RMSD and NSE by separating correlation error from relative variability error and bias in the means (Gupta et al., 2009).

#### 2.4.2. Similarity of Spatial Patterns Using the EOF Analysis

EOF analysis has been previously used as a means for comparing spatial patterns of modeled data with a reference data such as remotely sensed observations at the catchment scale (Koch et al., 2015). EOF analysis allows decomposition of a space-time data set to a set of time invariant orthogonal spatial patterns (EOFs; Perry & Niemann, 2007), as well as a set of loadings that represent the importance of each EOF at every time step (Koch et al., 2017). For comparing spatial similarity between modeled and reference data, Koch et al. (2015) performed the joint EOF analysis of a data matrix that includes spatial anomalies of reference and modeled data set at every time step. By removing the domain spatial mean from each grid cell at every time step, the EOF analysis becomes bias insensitive. The EOF-based similarity score introduced by Koch et al. (2015) is a measure of differences between the EOF loadings of modeled and reference data at every time step weighted by the variance contribution of a particular EOF. The EOF-based similarity score ($S^t_{\mathrm{EOF}}$) is computed as follows:

$$S^t_{\mathrm{EOF}} = \Sigma_{i=1}^{n} w_i \left| \left( \mathrm{load}_i^{B_t} - \mathrm{load}_i^{M_t} \right) \right| \tag{17}$$

where $w_i$ is the portion of the variance explained by the $i$th EOF and $\text{load}_i^B$ and $\text{load}_i^M$ are loadings of $i$th EOF at time $t$ for simulated soil moisture from ParFlow-CLM and a disaggregation method, respectively. Loadings are a matrix of size ($n \times n$) where $n$ is the number of time steps. Each row of a loading matrix corresponds to a particular EOF, and they express the contribution of each day of a time series to the direction of corresponding EOF. The total number of EOF is equal to $n$.

#### 2.4.3. Temporal Dependence

The memory timescale of soil moisture is the amount of time that it takes until the impact of a rain event on soil moisture temporal dynamics dissipates (Ghannam et al., 2016). This timescale typically ranges between a week to a few months depending on the size of a rainfall event, meteorological conditions, soil properties, and land surface characteristics (Ghannam et al., 2016). An autocorrelation function at multiple time lag intervals can be estimated to characterize temporal dependence of a time series. Delworth and Manabe (1988) analyzed soil moisture simulations of the Geophysical Fluid Dynamic Laboratory general circulation model and showed that the soil moisture autocorrelation function ($r(t)$) is exponential

$$r(t) = \exp\frac{-t}{\tau} \tag{18}$$

where $t$ is time and $\tau$ is the decay time scale that corresponds to a lag at which an autocorrelation function reduces to $1/e$ ($e$-folding time; Delworth & Manabe, 1988). We used the approach of Entin et al. (2000) to compute the decay time scale of a simulated soil moisture time series at every pixel by first computing an autocorrelation function at a 10-day lag interval and finding the slope of a linear regression fitted to the natural logarithm of autocorrelation functions and lag times (Entin et al., 2000). This slope is indicative of a decay time scale and is used as a measure of temporal dependence for comparing the performance of disaggregation methods at every pixel against ParFlow-CLM. Our preliminary analysis showed that the autocorrelation function becomes highly nonlinear at lags greater than 40 days.

## 3. Results

In the results that follow, comparisons are made across the four disaggregation approaches described along with their variants. To simplify the presentation, Table 2 summarizes all of the disaggregation models considered, along with their associated equations and key differences.

### 3.1. Does Topography Exert a First-Order Control on Soil Moisture Spatial Distribution?

Figure 2 presents results from the relative wetness index-based disaggregation alternative discussed earlier, which assumes that topography is the dominant driver in the disaggregation process. As can be seen in Figure 2, the TWI-based soil moisture disaggregation does not reproduce spatial variability of simulated soil moisture. Overall, this disaggregation approach performs better during the drydown periods and in the drier year (2006) than the wet periods. The daily NSE values become negative for catchment-averaged relative saturation values of greater than 0.4. These results are consistent with observations from catchments in temperate regions of Australia that showed a single wetness index cannot be representative of soil moisture distributions during wet and dry states of a catchment (Grayson et al., 1997). The fact that topography is better able to describe soil moisture spatial patterns during the drydown periods is also consistent with the two states hypothesis of Grayson et al. (1997). Based on this hypothesis, lateral flow processes control soil moisture spatial distribution during wet periods while local terrain and soil characteristics are the main contributors to soil moisture spatial pattern during the dry periods. The fact that the relative wetness index is not able to capture soil moisture spatial patterns during periods when lateral subsurface flow dominates (e.g., soil moisture peaks of 2010) might be related to some of the underlying assumptions of this index.

To assess the reasons behind the above results further, an EOF analysis is performed to extract the dominant spatial pattern of the top layer soil moisture simulations of ParFlow-CLM. As the first EOF of the soil moisture time series explained more than 97% of total variance in each simulation year (2006, 2008, and 2010), individual correlation coefficients between the first EOF and elevation, flow accumulation, slope and TWI are calculated (Mascaro et al., 2015). Results illustrate that the first EOF has the highest correlation with elevation (~−0.34) compared to other variables for all simulation years. This result confirms that topography is a marginally better descriptor of soil moisture spatial patterns compared to TWI with correlation coefficient of 0.3, with overall correlations relatively low for effective use as a disaggregation alternative as Figure 2 has shown.

**Table 2**
*Summary of Disaggregation Models*

| Method name | Equation(s) | Key differences |
|---|---|---|
| Relative wetness index | (1) | Disaggregation at every time step is performed using a constant rescaling ratio based on the topographic wetness index |
| TS: temporal stability | (2) | Linear regressions are developed between the time series of catchment mean soil moisture and soil moisture simulations at every pixel during the calibration period |
| TS.c: temporal stability model parameterized with soil moisture climatology | (2) | Similar to the TS method with the exception of using soil moisture climatology time series for model calibration |
| UAR1: univariate AR1 model | (3) to (8) | Incorporates soil moisture memory effect by estimating the lag-1 autocorrelation at every pixel from soil moisture ratio time series |
| UAR1.c: univariate AR1 model parameterized with soil moisture climatology | (3) to (8) | Similar to the UAR1 method with the exception of using soil moisture climatology time series at every pixel to estimate lag-1 autocorrelation |
| UAR1.SD: UAR1 model with the standard deviation rescaling | (3) to (10) | Similar to the UAR1 method with the exception that soil moisture rescaling is based on the catchment mean soil moisture and standard deviation |
| UAR1.cS: UAR1 model parameterized with soil moisture climatology and rescaling is based on standard deviation | (3) to (10) | Similar to the UAR1.SD method with the exception of using soil moisture climatology time series for autocorrelation estimation |
| MAR1: multivariate AR1 model | (8) and (11) | Incorporates lag-0 and lag-1 cross correlations between pixels in a domain |
| MAR1.c: MAR1 model parameterized with soil moisture climatology | (8) and (11) | Similar to the MAR1 method with the exception of using soil moisture climatology time series |
| MAR1.SD: MAR1 model rescaled with catchment-scale standard deviation | (10) and (11) | Similar to the MAR1 method with the exception of soil moisture rescaling based on the catchment-scale mean soil moisture and standard deviation |
| MAR1.cS: MAR1 model parameterized with soil moisture climatology and rescaling is based on standard deviation | (10) and (11) | Similar to the MAR1.SD with the exception of using soil moisture climatology time series |

### 3.2. Approximating Soil Moisture Spatial Variability Using Fine-Resolution Soil Moisture Simulations

Parameters of the temporal stability and the UAR1 and MAR1 models are estimated using the first 10 days of ParFlow-CLM soil moisture simulations in 2008. As can be seen in Figure 3, the temporal stability method performs better than the UAR1 and MAR1 models in 2006 and 2008 with some exceptions during wetter days of 2008 where daily NSE values are lower than the AR1 models. The UAR1 and MAR1 models perform best in 2010 compared to the temporal stability method. The decreasing trend of daily NSE values in 2010 coincides with increases in water table elevation (about 2 m) in the catchment caused by intense rainfall events. Comparisons among the disaggregation methods based on the KGE metrics indicate that the temporal stability method results in smaller correlations with observations (ParFlow-CLM) during wet days of 2008 and 2010. For the AR1 models, higher variability of the standard deviation bias ($\alpha$) in the dry year (2006) deteriorates the model performance.

While the temporal stability method has the best performance in 2006 and 2008 compared to AR1 models, this method does not preserve the soil moisture temporal persistence from previous time steps. Indeed, the pixel level lag-1 autocorrelations of disaggregated soil moisture from the temporal stability method are constant and equal to the lag-1 autocorrelation of catchment-averaged soil moisture, while they vary for the MAR1 and UAR1 models. As can be seen in Figure 3, UAR1 and MAR1 model performances are similar indicating that incorporating spatial association among pixels in the domain does not improve the disaggregation skill. Therefore, a simpler model based on the UAR1 approach is recommended.

One noticeable difference in the disaggregation results of the temporal stability and autoregressive methods compared to the relative wetness index is that NSE values are greater than 0.2 and 0.7, respectively, for the

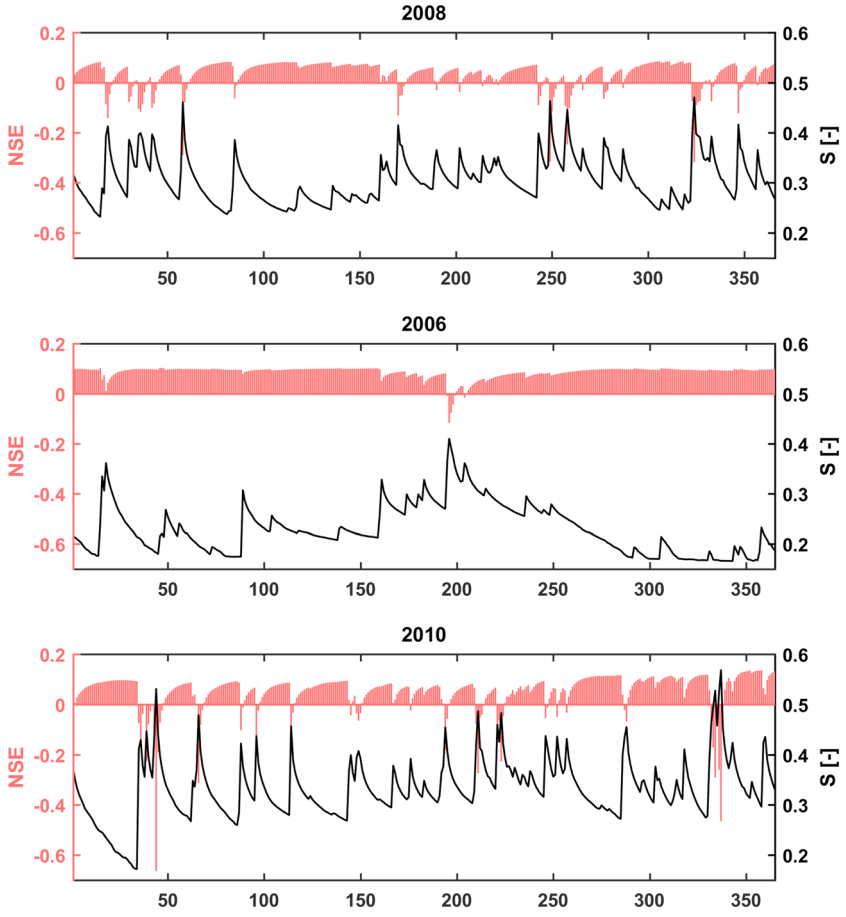


**Figure 2.** Daily NSE values of disaggregated top layer soil moisture using the relative wetness index disaggregation method. Catchment-averaged relative saturation (*S*) from ParFlow-CLM simulations in 2006, 2008, and 2010 are shown in black. This disaggregation approach performs better during the drydown periods as indicated by higher NSE values. NSE = Nash-Sutcliffe efficiency; CLM = Common Land Model.

validation periods. This means that the temporal stability method and particularly autoregressive models capture spatial distribution of ParFlow-CLM simulations very well using only 10 days of fine-resolution soil moisture data for their parameterizations. Total sum of similarity scores computed from the EOF analysis using all data for each year confirms the superior performance of the temporal stability method in 2008 and 2006 compared to the AR1 models as indicated by the smaller similarity scores (Figure 4a). However, the UAR1.c performs best in 2010 (Figure 4a).

The total number of model parameters in the temporal stability method is twice the AR1 models as it requires estimating the slope and intercept of a linear regression equation for every pixel. The UAR1 model only requires estimating the lag-1 autocorrelation for every pixel. Nevertheless, obtaining fine-scale soil moisture simulations across a large domain is computationally intensive using either approach. Next, we explore whether soil moisture simulations from a number of distributed cross sections in the domain can approximate soil moisture spatial distribution using the statistical approaches outlined above. It has been previously shown that the distributed cross sections that are almost perpendicular to a stream can capture subbasin-scale soil moisture dynamics (Ajami et al., 2016; Khan et al., 2014). The distributed cross-section approach is implemented in the semidistributed hydrologic modeling framework of SMART (Soil Moisture And Runoff simulation Toolkit) for computationally efficient hydrologic modeling (Ajami et al., 2016; Khan et al., 2013). If the disaggregation parameterization based on distributed cross sections works, the methods will be useful for mapping fine-scale soil moisture in semidistributed model simulations.

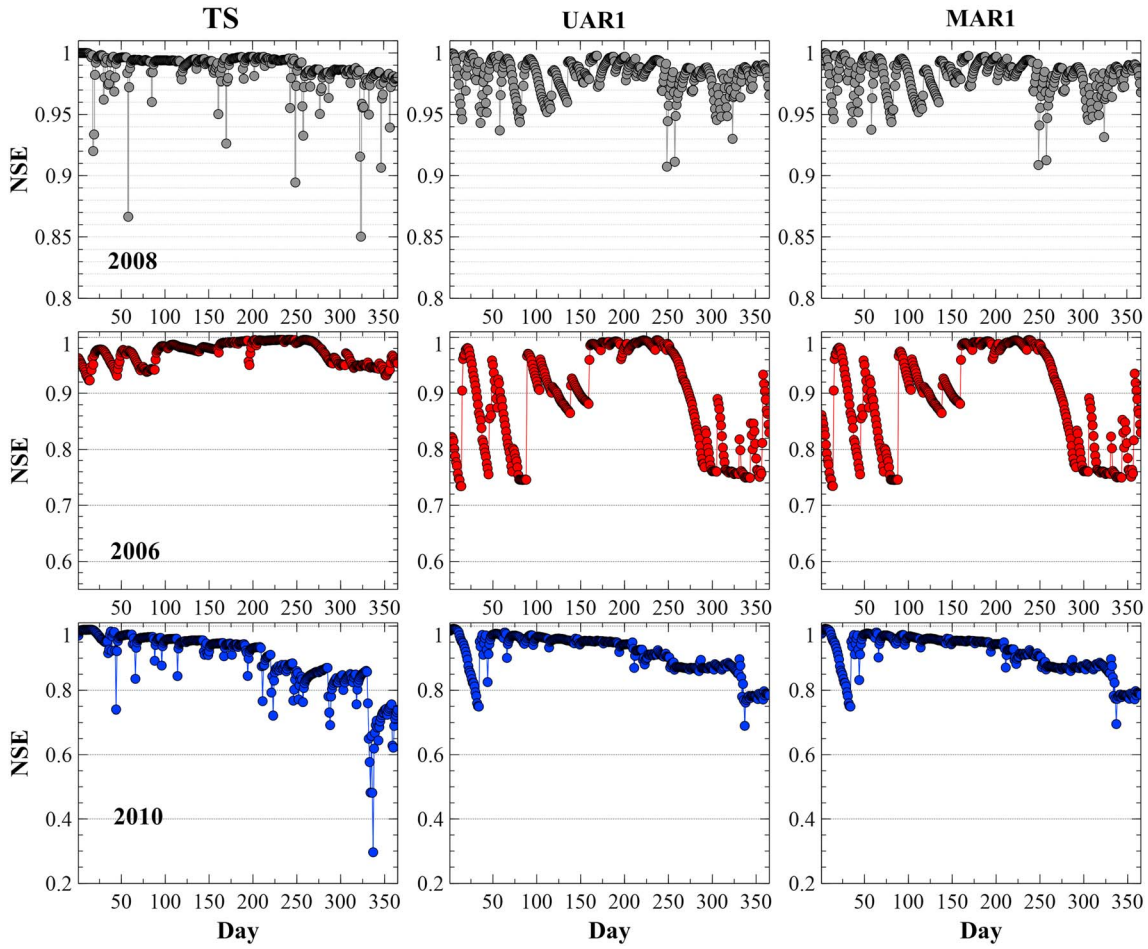


**Figure 3.** Daily NSE values of disaggregated soil moisture using the temporal stability (TS), UAR1, and MAR1 models. ParFlow-CLM simulations from 1 to 10 January of 2008 are used for calibrating the temporal stability and autoregressive models. NSE = Nash-Sutcliffe efficiency; UAR1 = univariate first-order autoregressive model; MAR1 = multivariate AR1 model; CLM = Common Land Model.

## 4. Discussions

### 4.1. Sensitivity of Disaggregated Soil Moisture to Model Parameterizations

In this section, we explore the impact of statistical model parameterization on accuracy of disaggregated soil moisture. First, the role of spatial distribution of observed samples on the statistical models performance is investigated by using soil moisture simulations from a set of distributed cross sections shown in Figure 1. Next, changes in the length of calibration period on predicted soil moisture are explored as estimating coefficients of linear regressions and autoregressive models requires a time series of fine-scale soil moisture simulations. This time series is referred here as representing a *calibration period*. Here we assessed the sensitivity of predicted soil moisture to the length of the calibration time series by choosing $m$ = 10, 20, 30, 40, 50, and 60 days of ParFlow-CLM simulations in 2008. Additional model parametrization is performed by obtaining a ($m$ = 10)-day soil moisture climatology based on ParFlow-CLM simulations in 2006, 2008, and 2010.

#### 4.1.1. Impact of Soil Moisture Spatial Sampling

To evaluate the impacts of spatial distribution of soil moisture simulations on disaggregation results, ParFlow-CLM soil moisture simulations across a series of cross sections (Figure 1) are extracted for 1–10 January 2008. The length of each cross section is 2,880 m and corresponds to 48 pixels of 60-m × 60-m size. The distance between two neighboring cross sections is 240 m. Parameters of the temporal stability and autoregressive models are estimated by first interpolating soil moisture values between the cross sections using the biharmonic spline method in MATLAB. Figure 5 shows daily disaggregation statistics for 2006, 2008, and 2010 for models constructed from the distributed cross sections. One noticeable feature is that model evaluation

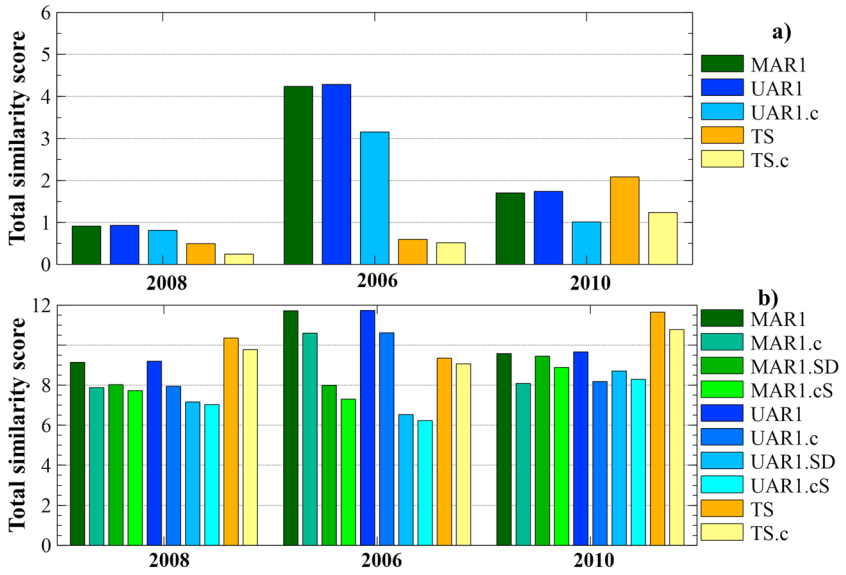


**Figure 4.** Yearly total similarity score from the EOF analysis using data from (a) all ParFlow-CLM pixels in the domain versus (b) data from distributed cross sections to parameterize the statistical models. For description of legend items refer to Table 2. EOF = empirical orthogonal function; CLM = Common Land Model.

metrics across all three statistical methods (temporal stability and univariate and multivariate autoregressive models) are decreased due to the lack of soil moisture simulations across the entire domain. Daily NSE values of the default model parametrizations (calibration is based on the first 10 days of 2008) are between 0.35 and 0.56 with the exception of the temporal stability method where NSE values reduce to 0.1 for certain days in 2010 (gray lines in Figure 5). Although disaggregation model parameterization using the distributed cross sections reduces NSE by 50% in some cases, all the statistical methods perform better than the relative wetness index-based disaggregation (Figure 2).

Soil moisture rescaling based on the spatial standard deviation and catchment mean soil moisture (green lines in Figures 5 and 6) significantly improves model predictions relative to the catchment mean rescaling. Improved performance of the AR1 models particularly those that adjust predictions based on the standard deviation is more evident using the KGE metrics compared to NSE (Figure 6). According to the KGE metrics, the standard deviation-based rescaling improves the correlation structure of predicted soil moisture against observations as well as reducing variability of the daily spatial standard deviation bias. These improvements are reflected by higher and less variable daily KGE values of AR1 models (Figure 6). Similar to Figure 3, performances of the UAR1 and MAR1 models are similar indicating that spatial association among the pixels in the domain does not lead to improved performance of the contemporaneous MAR1 model.

NSE values of all the statistical models for the cross-sections pixels are greater than 0.75 in 2006 and 2008 (Figure 7). In 2010, a decreasing trend in daily NSE values caused by increases in water table elevation reduces the NSE of the AR1 and temporal stability methods to 0.65 and 0.1, respectively. While at the interpolated pixels NSE values are smaller (~0.35), the statistical disaggregation approaches perform better than the relative wetness index approach at these locations with lower NSE values (Figure 2). Furthermore, soil moisture climatology parameterization in addition to the standard deviation rescaling improves AR1 model predictions particularly over the interpolated pixels (Figure 7). Ranges of RMSD values across all years and various disaggregation alternatives are between 0.016 and 0.03 $m^3/m^3$.

Comparing predicted soil moisture spatial patterns from models parametrized based on the distributed cross sections also confirms that the autoregressive methods perform best in 2008 and 2010 relative to the temporal stability method (Figure 4b). In 2006, the temporal stability method performs better than some variants of the autoregressive models for reasons that are addressed later.

#### 4.1.2. Sensitivity to the Length of Calibration Period

Sensitivity analysis results using the calibration period of 10, 20, 30, 40, 50, and 60 days (using data from ParFlow-CLM in 2008) for the distributed cross-sections parameterization reveal that calibration period of

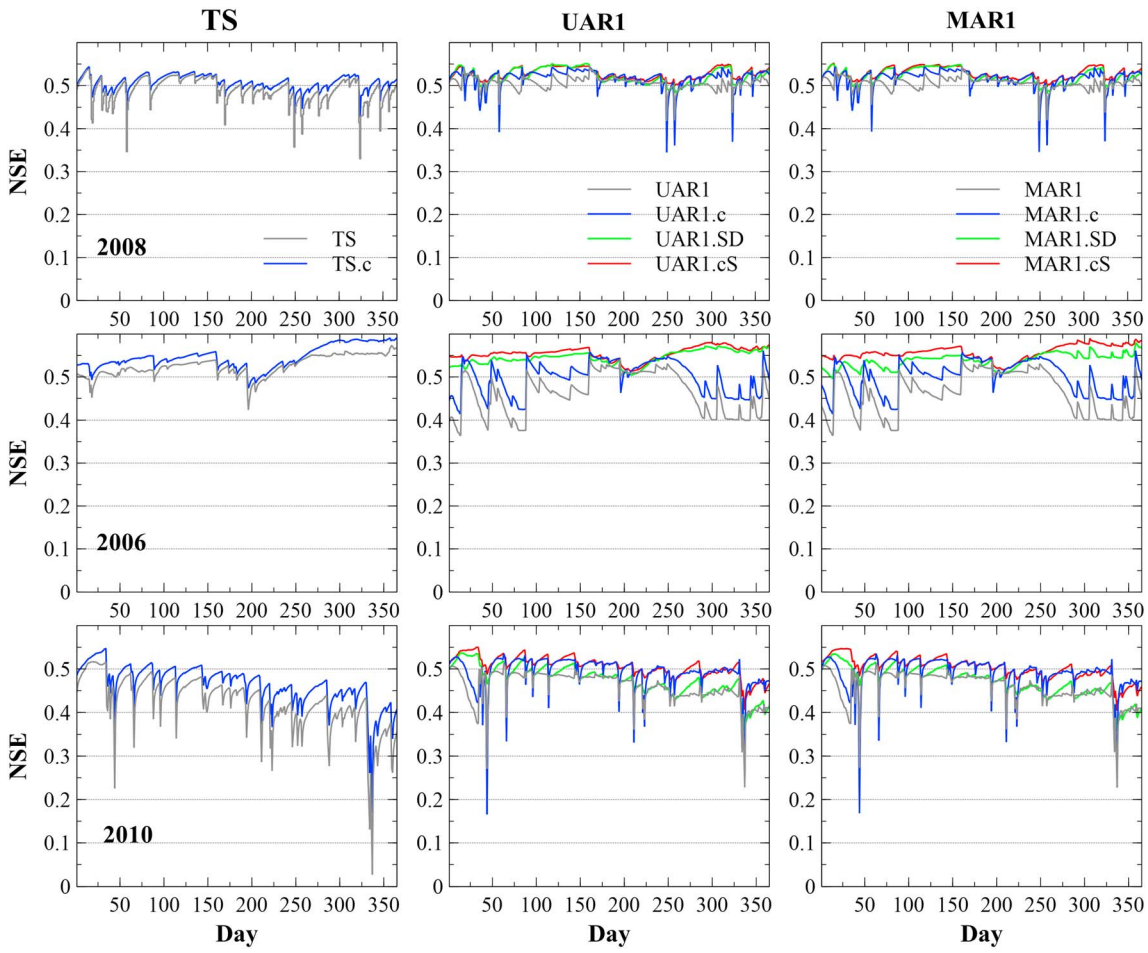


**Figure 5.** Daily NSE values of disaggregated soil moisture based on the temporal stability (TS), UAR1, and MAR1 models using ParFlow-CLM simulations of 1–10 January 2008 from distributed cross sections for calibration. Description of legend items are in Table 2. NSE = Nash-Sutcliffe efficiency; CLM = Common Land Model.

10 days is sufficient for capturing soil moisture dynamics particularly in 2006 and 2008 (Figure 8). To illustrate this, mean daily NSE values of each disaggregation method calibrated to a particular calibration period are calculated and summarized in boxplots for validation years. Each boxplot of Figure 8 shows ranges of mean NSE values from 10 disaggregation methods (Table 2) including temporal stability, temporal stability based on the soil moisture climatology, default AR1 model, AR1 model based on the soil moisture climatology, AR1 model based on the standard deviation rescaling, and AR1 model based on the soil moisture climatology and standard deviation rescaling. Note that the AR1 category includes both univariate and multivariate models. As can be seen in Figure 8 increasing the calibration period does not significantly improve model predictions, and it even increases the ranges of daily NSE values and number of extreme outliers. The outliers are from the MAR1 models calibrated to 60 days. In general, UAR1.cS and/or MAR1.cS models have the highest NSE.

Performances of calibrated statistical models using a 10-day soil moisture climatology data are shown in Figures 4–7. As can be seen in Figure 4a, the temporal stability method based on soil moisture climatology using the entire domain data has the best similarity score of the models considered in this study in 2006 and 2008, while the UAR1 model based on soil moisture climatology is the best model in 2010. This result suggests that the impact of soil moisture memory becomes more important in 2010 as this year is significantly wetter than 2006 and 2008. For the distributed cross-sections parameterization, the UAR1.cS model predictions (calibrated by the soil moisture climatology and rescaled by the standard deviation) are the best. Calibration based on the soil moisture climatology compared to the default parameterization improves soil moisture predictions in all the statistical methods (Figure 4). However, the standard deviation rescaling is

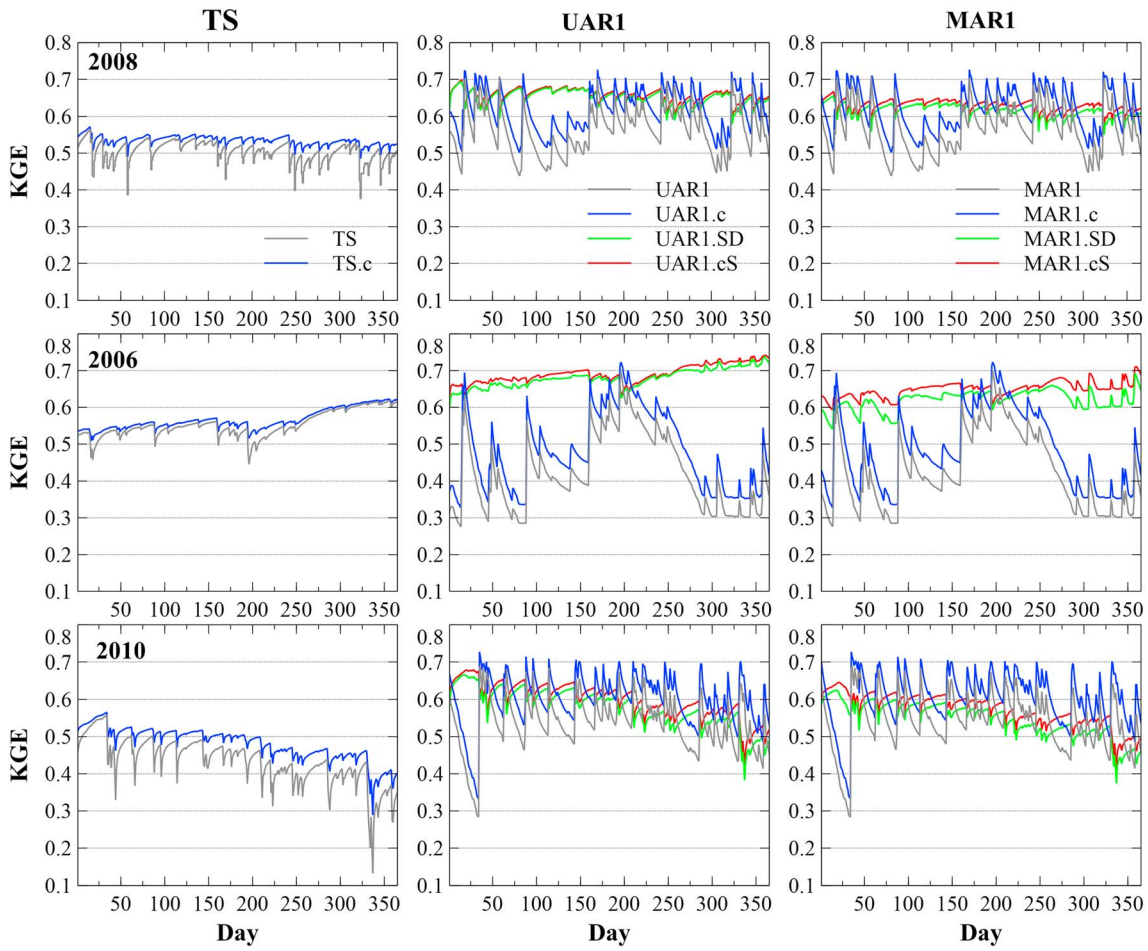


**Figure 6.** Daily KGE values of disaggregated soil moisture based on the temporal stability (TS), UAR1, and MAR1 models using ParFlow-CLM simulations of 1–10 January 2008 from the distributed cross sections for calibration. Descriptions of legend items are in Table 2. KGE = Kling-Gupta efficiency; CLM = Common Land Model.

more impactful than the soil moisture climatology parametrization in the AR1 models particularly during the dry year (2006) (Figures 4 and 5). For the distributed cross-section approach, calibration based on soil moisture climatology and standard deviation rescaling improves soil moisture predictions of interpolated pixels across all the validation years. However, predictions at cross-section pixels do not improve during 2006 and 2008. Indeed, the cross-section pixels with the standard deviation rescaling and default parameterization (1–10 January 2008) have higher NSE than the models calibrated by soil moisture climatology and standard deviation rescaling (Figure 7).

#### 4.1.3. Sensitivity to the Timing of a Calibration Period

A series of model calibration experiments are performed to assess sensitivity of univariate AR1 models predictions to the 10-day period. A total of 357 calibration periods is specified by considering a 10-day moving window starting from 1 January 2008 to the end of the year. For soil moisture climatology calibrations, average of soil moisture simulations from 2006, 2008, and 2010 is used. The calibration experiments are implemented for the default UAR1 parameterization, UAR1.c, and UAR1.SD models. Therefore, 1,071 (357 × 3) UAR1 models are developed to disaggregate daily catchment averaged soil moisture for 2006, 2008, and 2010. Figure 9 shows minimum, maximum, 25th, 50th, and 75th percentiles of the daily KGE values from each model calibrated to a different 10-day period. As can be seen in Figure 9, standard deviation rescaling significantly reduces sensitivity of soil moisture predictions to the calibration period, and ranges of KGEs are larger in 2006 and 2010 validation periods. Sensitivity of model predictions for the UAR1 and UAR1.c parameterizations is lowest during drier periods as the highest KGE corresponds to calibration periods with smaller catchment mean soil moisture.

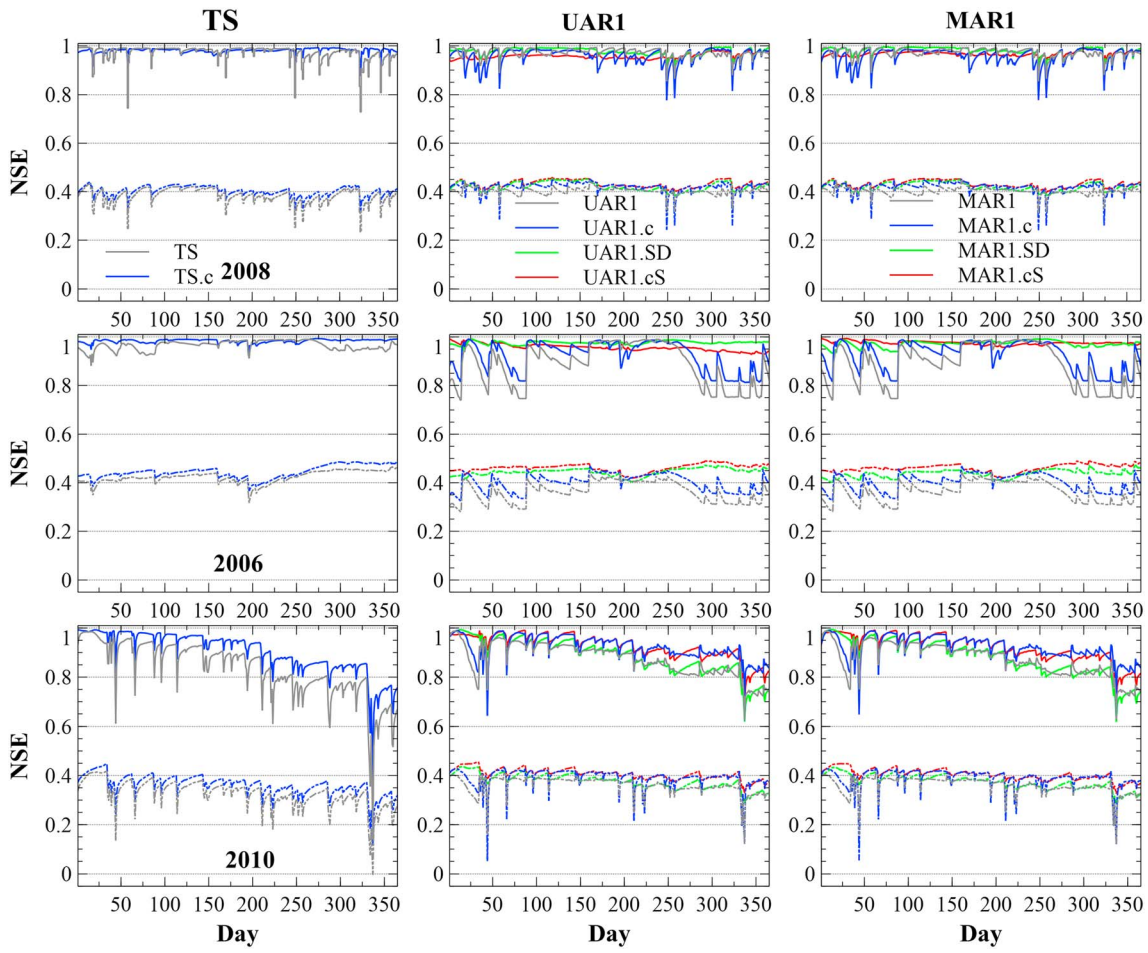


**Figure 7.** Daily NSE values of disaggregated soil moisture based on the temporal stability (TS), UAR1, and MAR1 models using ParFlow-CLM simulations of 1–10 January 2008 from the distributed cross sections for calibration. The solid lines are NSE of distributed cross-sections pixels, and the dashed lines represent NSE of interpolated pixels. Descriptions of legend items are in Table 2. NSE = Nash-Sutcliffe efficiency; CLM = Common Land Model.

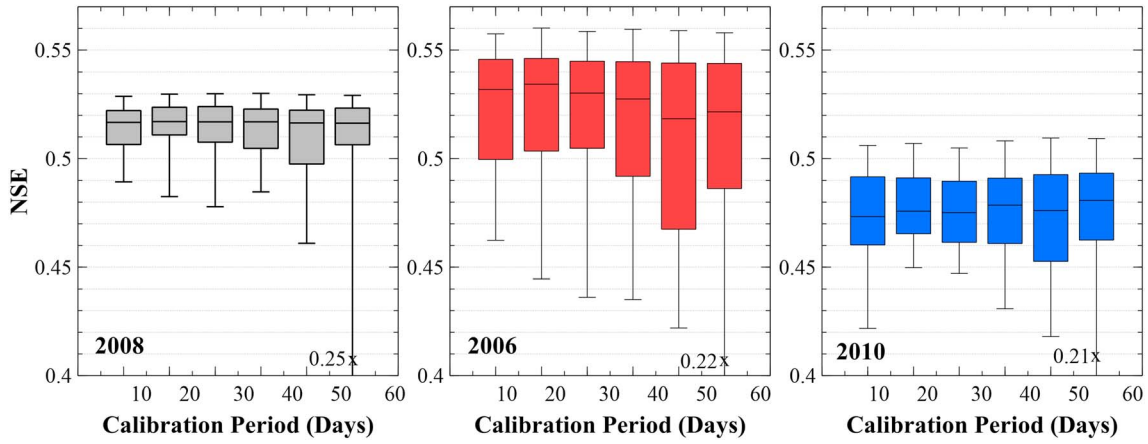


**Figure 8.** Sensitivity of statistical disaggregation methods to the length of calibration period. Each boxplot presents the ranges of mean NSE values from 10 disaggregation methods parameterized from the distributed cross-sections simulations. The disaggregation methods are temporal stability, temporal stability with soil moisture climatology, univariate and multivariate AR1 models using default parameterization, soil moisture climatology, rescaling based on spatial standard deviation, and parameterization based on soil moisture climatology and rescaling based on spatial standard deviation. NSE = Nash-Sutcliffe efficiency; AR1 = first-order autoregressive model.

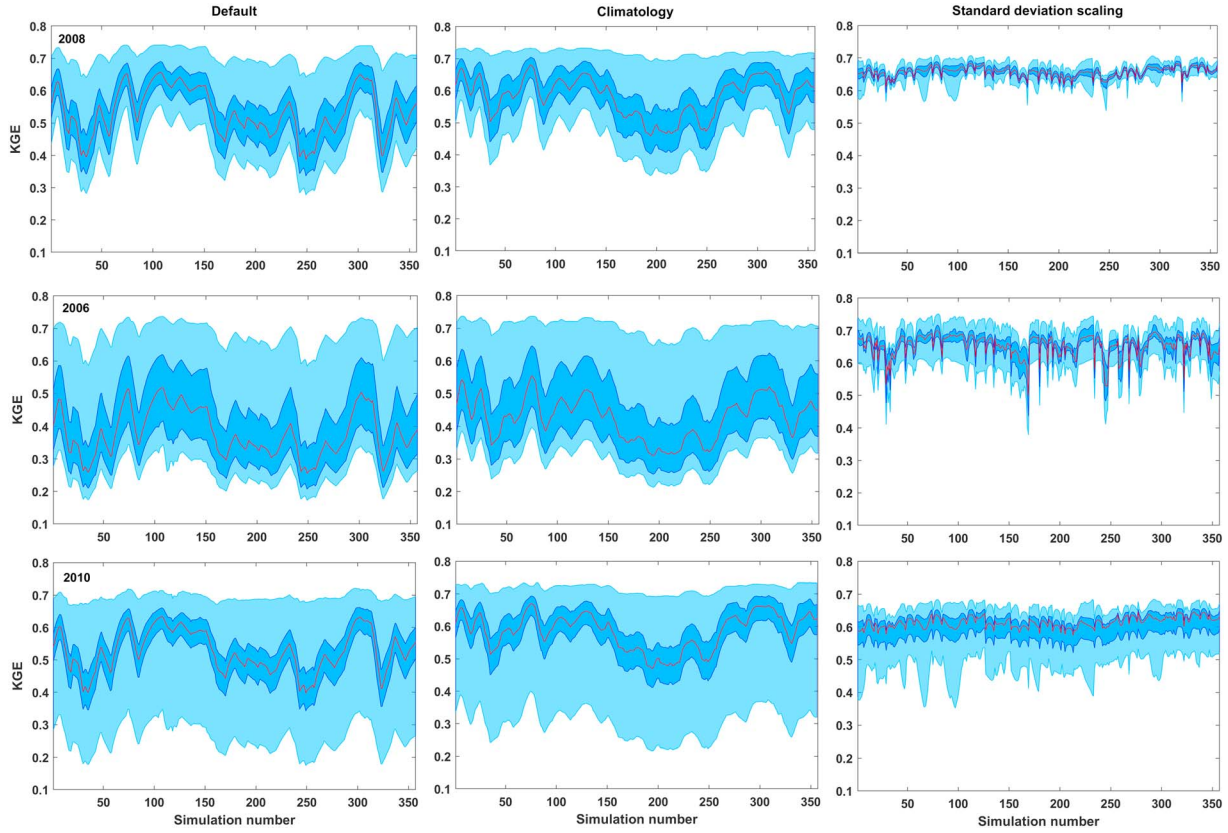


**Figure 9.** Ranges of daily KGE values of soil moisture predictions for a given simulation year obtained from three UAR1 models calibrated to a different 10-day period using 2008 and climatology time series. The AR1 models are UAR1, UAR1.c, and UAR1.SD. Minimum and maximum KGE values are shown in light blue, and 25th and 75th percentiles are shown in dark blue. The 50th percentiles of daily KGE values are in red. KGE = Kling-Gupta efficiency; UAR1: univariate AR1 model; AR1 = first-order autoregressive model; UAR1.c = univariate AR1 model parameterized with soil moisture climatology; UAR1.SD = UAR1 model with the standard deviation rescaling.

### 4.2. Overall Performance of Disaggregation Models

As the goal of disaggregation is to reduce the computational demand of fine-scale simulations, the next logical step is to identify a disaggregation method that well represents soil moisture spatial variability in a range of conditions using multiple performance measures. To perform this evaluation, all the models formulated from the distributed cross sections are ranked based on the four evaluation metrics including mean NSE, KGE, $r$, and $\alpha$ using data from 2006, 2008, and 2010 (Best et al., 2015). For a given evaluation metrics, the score of 10 is assigned to the best performing model and the worst performing model is given the score of 1. These rankings are summed across all the metrics to obtain the total rank for a given disaggregation alternative. As it is shown in Figure 10, the UAR1 model performs best (has the largest rank) particularly when it is calibrated to soil moisture climatology and predictions are rescaled by the catchment mean soil moisture and standard deviation. Incorporating a more complex autocorrelation structure in the MAR1 models does not improve soil moisture predictions compared to the univariate models.

The temporal stability approach tends to perform better than the AR1 models with the default and soil moisture climatology parameterizations during the 2006 (dry) validation year. However, AR1 models typically perform better than the temporal stability method during years with average or wetter conditions (2008 or 2010).

Comparing ranges of daily spatial variance of soil moisture across the 15 statistical disaggregation models against observations confirms that the entire domain parameterizations well resemble the spatial patterns of observations (Figure 11). The best performing methods based on the entire domain data are the temporal stability method in 2006 and univariate AR1 models based on soil moisture climatology in 2008 and 2010. For the distributed cross sections, the UAR1 models based on the joined soil moisture climatology and standard

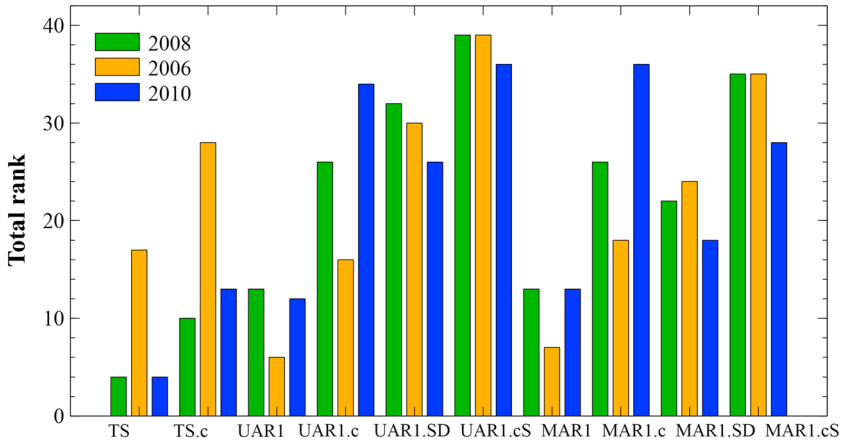


**Figure 10.** Ranking of 10 disaggregation methods parameterized based on the distributed cross section simulations. The best performing model has the highest rank. TS = temporal stability.

deviation rescaling or standard deviation rescaling perform better than other alternatives particularly in 2006 and 2008. The numbers of outliers are larger in 2010 across all the models.

Finally, the temporal dependence of disaggregation methods for 2006, 2008, and 2010 is compared with ParFlow-CLM simulations using the temporal dependence metrics described in section 2.4.3. As can be seen in Figure 12, the temporal stability method results in a constant decay time scale across all grid cells equal to the catchment averaged soil moisture decay time scale. Among the autoregressive models, the UAR1 model calibrated to soil moisture climatology and adjusted to soil moisture standard deviation better resembles cumulative probability distribution of decay time scales estimated for each pixel. As expected, the decay time scale of a drier year (2006) is longer than 2008 and 2010. The decay time scale distribution in 2010 is larger than the average year (2008). This result highlights the role of precipitation amount on impacting soil moisture memory time scale.

### 4.3. Comparing the AR1 Model Performance Against the TOPMODEL Approach

The TOPMODEL soil moisture distribution approach based on the catchment averaged soil moisture deficit and TWI distribution has been widely used in hydrologic and land surface models. The TOPMODEL estimates soil moisture deficit at every pixel by assuming a steady state condition and an exponential decline of hydraulic conductivity with depth:

$$D_{i,j}(t) = \overline{D}(t) - m\left[\left(TWI_{i,j} - \overline{TWI}\right) - \left(\ln T_0 - \overline{\ln T_0}\right)\right] \tag{19}$$

where $D_{i,j}$ is the soil moisture deficit at pixel $i,j$ and time $t$, $m$ is a constant scaling parameter, $TWI_{i,j}$ is the topographic wetness index of pixel $i,j$, $\overline{D}$ and $\overline{TWI}$ are catchment-averaged soil moisture and TWI, respectively, $T_0$ is the local transmissivity at saturation, and $\overline{T_0}$ is catchment-averaged transmissivity (Beven, 1997). We compared soil moisture predictions from the univariate AR1 model with the TOPMODEL disaggregation by assuming a homogenous soil (the second term on the right-hand side of equation (19) becomes zero) and replacing soil moisture deficit by soil moisture.

Catchment-scale soil moisture disaggregation from the TOPMODEL approach with a constant rescaling parameter results in poor model predictions (negative daily NSE values). To improve the model performance, parameter $m$ is estimated for every pixel using ParFlow-CLM simulations from 1 to 10 January 2008. Distributed parameter values ($m$) estimated from the entire domain simulations improve soil moisture predictions in 2006 relative to the UAR1 model, but results are worse than the temporal stability method (Figure 13). This outcome is related to the differences in parameterizations between the TOPMODEL and temporal stability method. The TOPMODEL assumes that the relationships between the catchment-averaged soil moisture and local-scale soil moisture have a slope of 1, and the only changing parameter is the local TWI fixed at every time step. For the distributed cross-section cases, the UAR1.SD is the best performing model as the

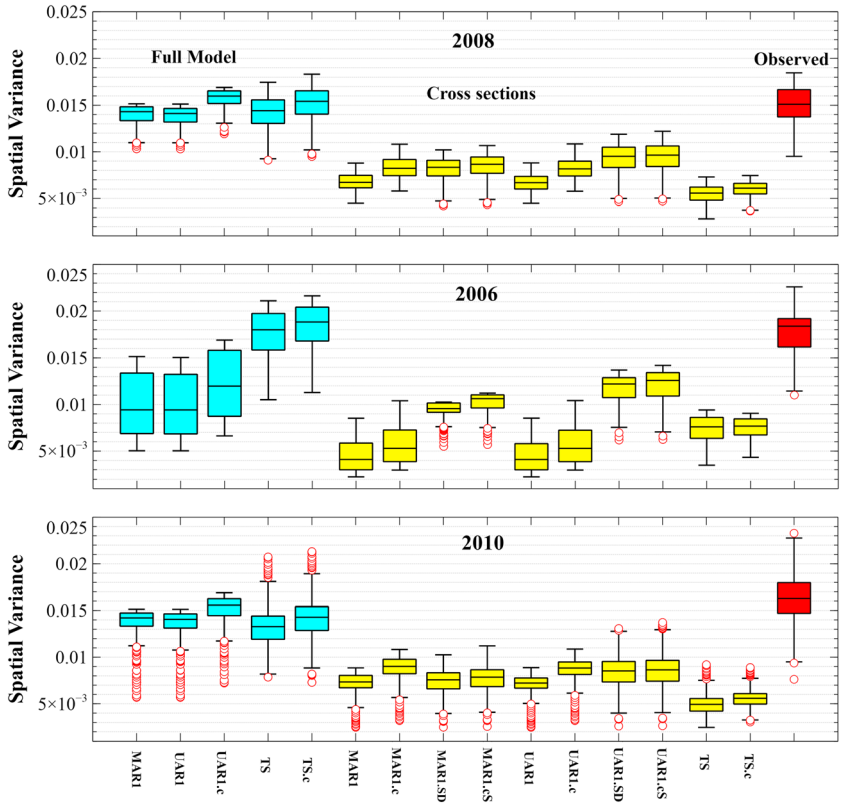


**Figure 11.** Spatial variance of predicted daily soil moisture from the 15 statistical models parameterized using the full domain data and distributed cross sections. The red boxplots show the range of observed spatial variance based on ParFlow-CLM simulations. CLM = Common Land Model. TS = temporal stability; TS.c = temporal stability model parameterized with soil moisture climatology; UAR1 = univariate AR1 model; UAR1.c = univariate AR1 model parameterized with soil moisture climatology; UAR1.SD = UAR1 model with the standard deviation rescaling; UAR1.cS = UAR1 model parameterized with soil moisture climatology and rescaling is based on standard deviation; MAR1 = multivariate AR1 model; MAR1.c = MAR1 model parameterized with soil moisture climatology; MAR1.SD = MAR1 model rescaled with catchment scale standard deviation; MAR1.cS = MAR1 model parameterized with soil moisture climatology and rescaling is based on standard deviation.

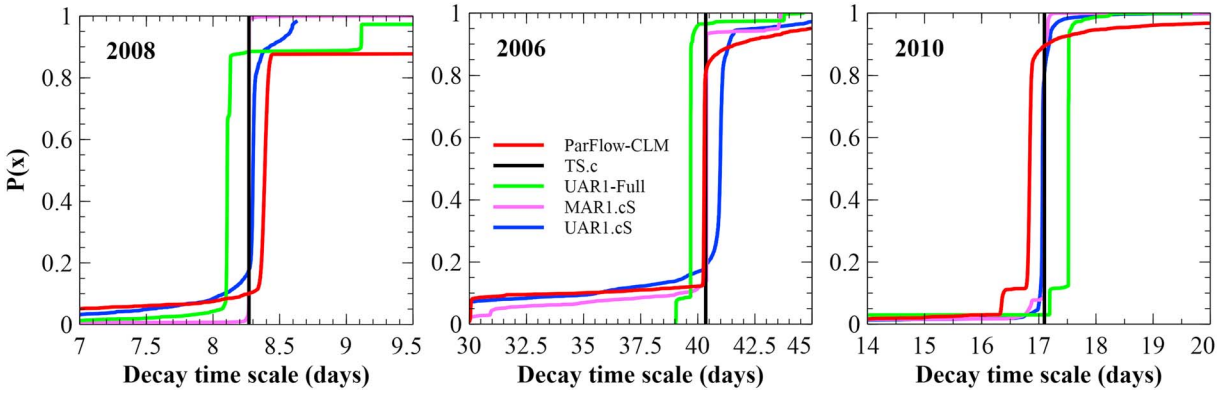


**Figure 12.** Cumulative distribution function of pixel-based soil moisture decay time scale for ParFlow-CLM simulation, temporal stability method calibrated to soil moisture climatology, and UAR1.cS and MAR1.cS models. All models are parameterized based on soil moisture simulations from distributed cross sections except for the UAR1-Full model that includes data from the entire ParFlow-CLM domain. The temporal stability method results in a constant decay time scale equal to the decay time scale of catchment-averaged soil moisture time series. CLM = Common Land Model; UAR1.cS: UAR1 model parameterized with soil moisture climatology and rescaling is based on standard deviation; MAR1.cS = MAR1 model parameterized with soil moisture climatology and rescaling is based on standard deviation; UAR1 = univariate AR1 model.

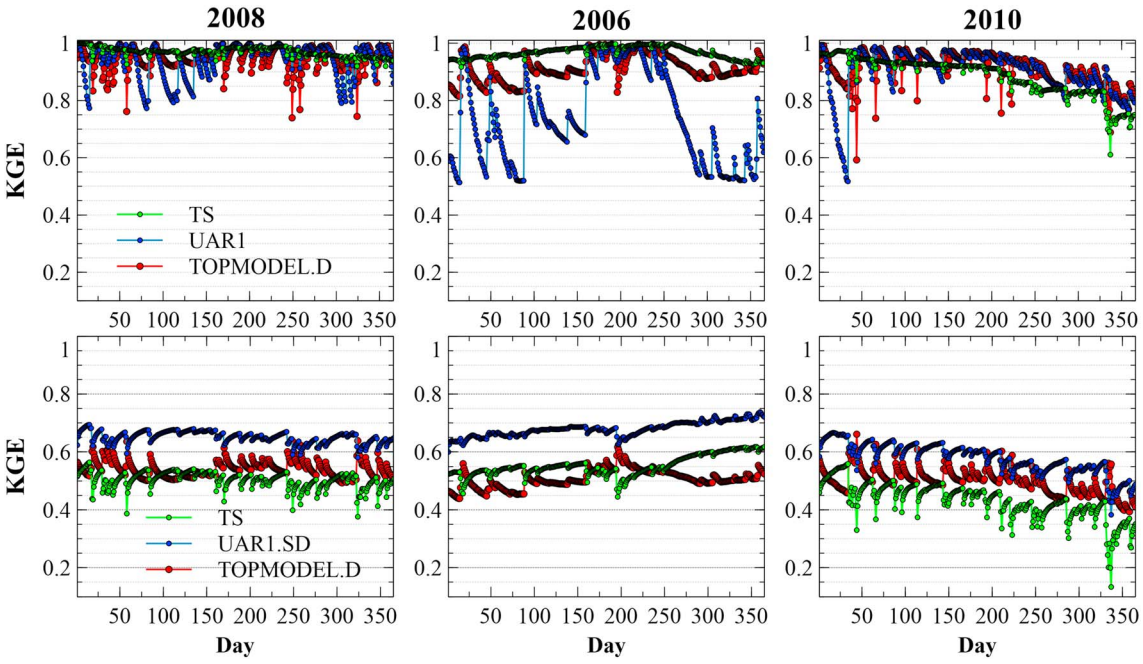


**Figure 13.** Daily KGE values of soil moisture predictions from the temporal stability method, UAR1, UAR1.SD model and TOPMODEL with distributed parameter values (TOPMODEL.D) calibrated to a 10-day calibration period in 2008. While the temporal stability model produces the best predictions in 2006 and 2008 using the entire domain data for its parameterization (top row), the UAR1 model produces the best results using the distributed cross sections (bottom row). KGE = Kling-Gupta efficiency; UAR1 = univariate AR1 model; UAR1.SD = UAR1 model with the standard deviation rescaling; TOPMODEL = a TOPography based hydrological MODEL; TS = temporal stability.

time-varying ratio of local soil moisture to catchment-averaged value at every time step cannot be captured using the non-time-varying TWI indicators in TOPMODEL (Figure 13).

### 4.4. Application of AR1 Models in Semidistributed Hydrologic Modeling

Semidistributed hydrologic models such as SMART delineate a series of subbasins in a particular catchment and has multiple approaches for delineating the computational elements in a subbasin. In SAMRT, these elements are either series of two-dimensional distributed cross-sections perpendicular to a stream or equivalent cross sections (ECSs) representative of each hillslope in a subbasin (Ajami et al., 2016). In the case of distributed pixel-based cross sections, SMART delineates a series of distributed cross sections across a subbasin and obtains model parameters per pixel (Figure S1 in the supporting information). By adjusting the distance between the cross sections, this formulation can represent a fully distributed simulation case. For the ECSs approach, SMART first delineates a series of cross sections per hillslope and then aggregates hillslope parameters (e.g., slope, vegetation, and soil types) for every landform (HRU) to formulate an ECS for every hillslope. In SMART, these HRUs are delineated based on variation in topographic and geomorphologic descriptors of the entire catchment in relation to distance from a stream (Khan et al., 2013) and are classified as upslope, midslope, footslope, and alluvial flats landforms. The ECS formulation in SMART substantially reduces the computational time by decreasing the number of cross sections from 67 from the fully distributed pixel based to 3. SMART assumes a uniform soil moisture distribution across regions with similar hydrologic response units. Therefore, there is a need to disaggregate subbasin soil moisture values to fine resolution for certain applications.

Here we examined whether the autoregressive coefficient ($A$) estimated from the distributed cross sections using ParFlow-CLM simulations (Figure 1) can approximate fine-resolution soil moisture using subbasin-averaged soil moisture values of the three ECSs approach for every time step. As the two-dimensional unsaturated zone hydrologic model (U3M-2D; Tuteja et al., 2004) in SMART is different than ParFlow-CLM, another reference data are required to assess UAR1 model performance. As a result, a fully distributed cross-section simulation with 67 cross sections is performed using SMART. U3M-2D solves the two-dimensional Richards equation for soil moisture predictions and uses daily potential evapotranspiration to estimate

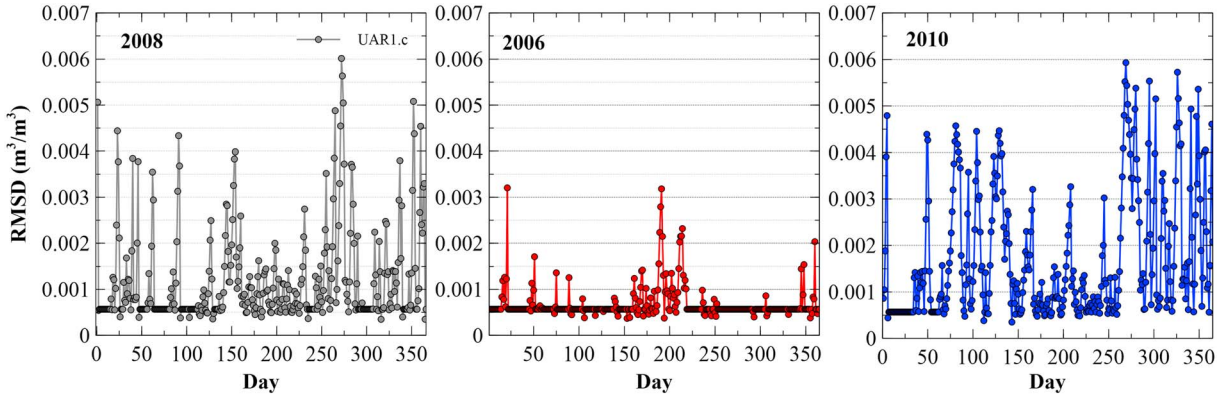


**Figure 14.** Daily RMSD values of disaggregated catchment mean soil moisture using mean soil moisture values of three ECSs simulations at every time step and ParFlow-CLM derived *A* coefficient from the UAR1.c approach. Fine scale soil moisture values of SMART distributed pixel-based simulations are used as the virtual observations. RMSD = root-mean-square difference; UAR1.c = univariate AR1 model parameterized with soil moisture climatology; ECS = equivalent cross section; CLM = Common Land Model; SMART = Soil Moisture And Runoff simulation Toolkit.

evapotranspiration, and current version of SMART does not have a groundwater module. Despite this limitation, previous investigations have shown that the ECS formulation is able to capture subbasin scale (Ajami et al., 2016; Khan et al., 2014) and catchment mean soil moisture temporal dynamics (Khan et al., 2018) compared to observations obtained from soil moisture monitoring probes or satellite observations, respectively. In addition, runoff simulations from the three ECSs approach without any calibration were comparable to observed discharge and simulations from four calibrated conceptual models at catchment scale (Khan et al., 2018).

To be consistent with ParFlow-CLM, daily reference potential evapotranspiration was estimated using hourly forcing data of ParFlow-CLM and the soil depth over the catchment was assumed at 5 m. This depth represents the CLM exchange zone with ParFlow. Soil moisture disaggregation results demonstrate that the ParFlow-CLM-derived *A* coefficient with subbasin soil moisture values from the three ECSs approach produces similar soil moisture distributions to the fully distributed pixel-based cross-section formulations of SMART as indicated by small daily RMSD values (Figure 14). This result indicates that SMART has the potential to derive parameters of UAR1 models and due to its computational efficiency has the potential for large scale simulations and derivation of soil moisture disaggregation parameters. In the next step, sensitivity of UAR1 model to catchment characteristics such as topography, horizontal, and vertical subsurface heterogeneity using SMART will be explored.

### 4.5. Sensitivity of a UAR1 Model to Catchment Characteristics Using SMART

To assess sensitivity of a UAR1 model to catchment characteristics such as steepness, horizontal, and vertical subsurface heterogeneity, five simulation scenarios are designed using Baldry data as the basis for model simulations. The details of scenarios are as follows: (I) Scenario 1—homogenous subsurface with the existing land cover. This scenario represents the baseline condition and is similar to the ParFlow-CLM set-up. (II) Scenario 2—similar to scenario 1 with the exception of multiplying catchment elevation by a factor of 10 to increase the slope. (III) Scenario 3—similar to scenario 1 with the exception of representing the subsurface using a randomly generated soil texture field with four soil texture classes: sand, loamy sand, sandy loam, and loam (Figure S2a). (IV) Scenario 4—similar to scenario 1 with the exception of representing the subsurface by four soil texture classes that follow topography: sand, loamy sand, sandy loam, and loam (Figure S2b). (V) Scenario 5—similar to scenario 1 with the exception of representing the subsurface with four vertical soil layers of different texture. These texture classes and their corresponding thicknesses from top to the bottom layers are as follows: sand (0.3 m), silt (0.3 m), silty loam, (0.4 m) and clay loam (4 m).

For every scenario, three model simulations are performed: (I) a fully distributed model simulations by discretizing the catchment to 67 cross sections perpendicular to the stream to cover the entire catchment. These simulations are used as virtual observations for comparison with the UAR1 model; (II) a semidistributed model simulation by discretizing the catchment to 15 cross sections, 3 cross sections

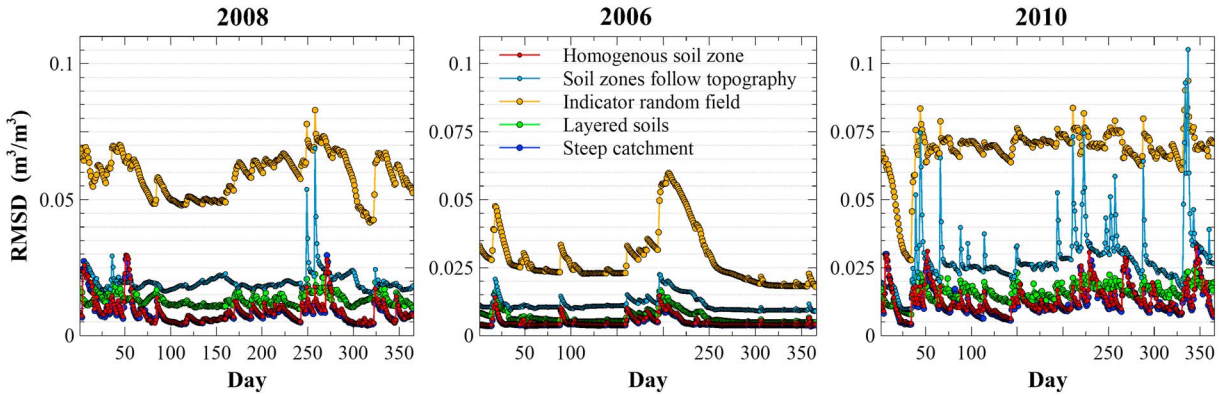


**Figure 15.** Daily RMSD values of UAR1.c disaggregated soil moisture fields against the fully distributed SMART simulations for every scenario. RMSD = root-mean-square difference; UAR1.c = univariate AR1 model parameterized with soil moisture climatology; SMART = Soil Moisture And Runoff simulation Toolkit.

for the headwater, and 6 cross sections for each side slope (Figure S1). These cross sections are used to develop the UAR1 model A matrix; and (III) an ECS approach by delineating one ECS per hillslope (headwater, right bank and left bank). These ECSs are used to obtain the catchment mean soil moisture for soil moisture disaggregation.

Comparing daily RMSD values of each scenario for 2006, 2008, and 2010 simulation years shows that horizontal and vertical heterogeneity of subsurface parameters increases RMSD of the disaggregated soil moisture by the UAR1 model (Figure 15). The largest error is caused by the random indicator field followed by the four soil zones field that follow topography scenario and layered soils scenario. The magnitude of RMSD for the steep catchment is the same as the scenario 1 (Figure 15).

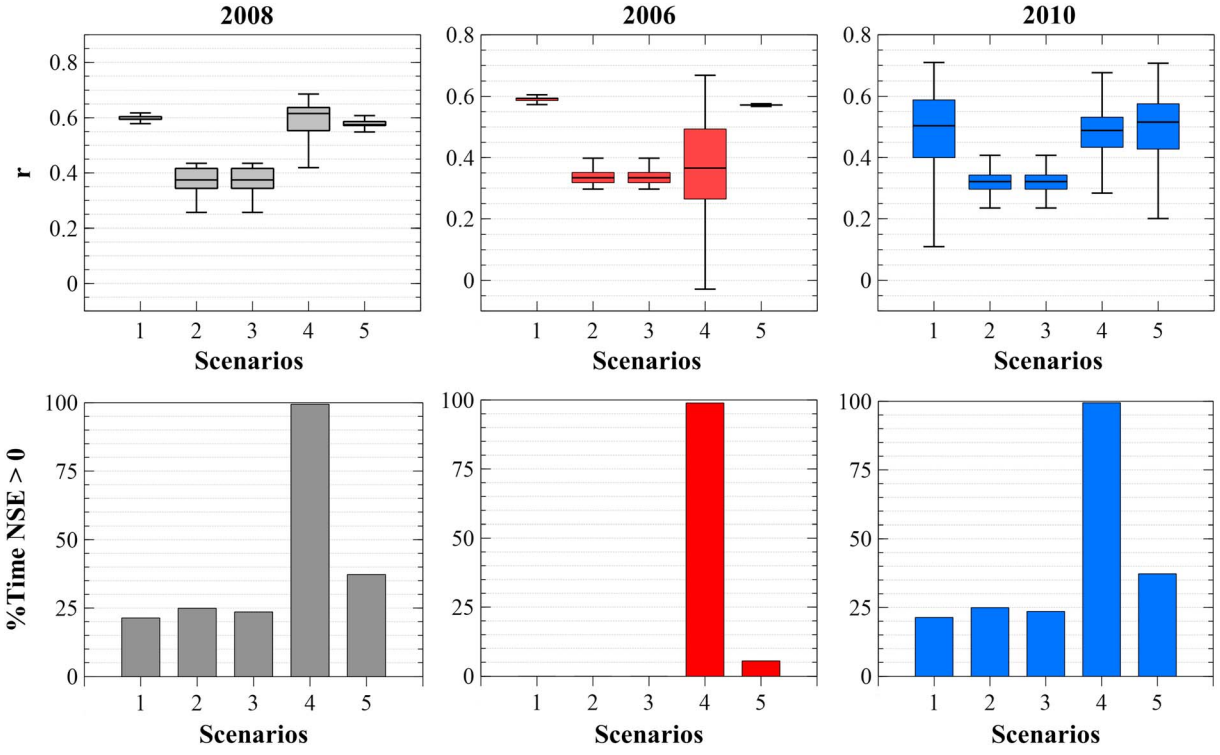


**Figure 16.** Ranges of daily correlation values between spatially distributed soil moisture fields from the UAR1.c model and SMART fully distributed simulations (top row). Percentage of the time in each simulation year where NSE values of the disaggregated soil moisture field against the fully distributed SMART simulations is greater than 0 (bottom row). Scenarios 1 through 5 represent the following: 1 (homogenous), 2 (steep), 3 (indicator random field), 4 (soil zones follow topography), and 5 (layered soils). UAR1.c = univariate AR1 model parameterized with soil moisture climatology; SMART = Soil Moisture And Runoff simulation Toolkit; NSE = Nash-Sutcliffe efficiency.

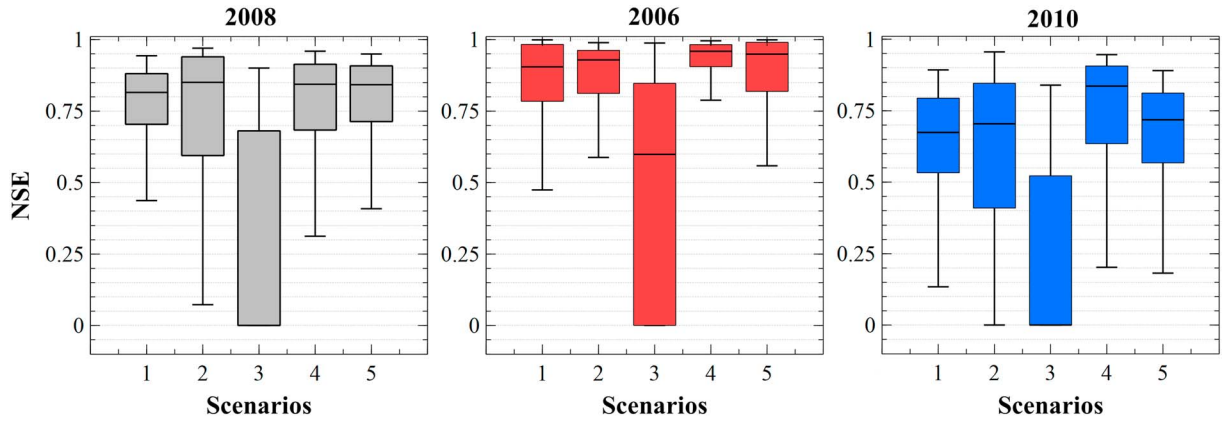


**Figure 17.** Ranges of NSE values of disaggregated soil moisture time series at every pixel against the fully distributed SMART simulations for each scenario. Scenarios 1 through 5 represent the following: 1 (homogenous), 2 (steep), 3 (indicator random field), 4 (soil zones follow topography), and 5 (layered soils). NSE = Nash-Sutcliffe efficiency; SMART = Soil Moisture And Runoff simulation Toolkit.

One noticeable difference between these simulations and ParFlow-CLM simulation is that lateral connectivity between neighboring cross sections in the fully distributed SMART simulations are ignored, and each cross section is simulated independent of its neighboring cross sections. This has degraded the UAR1 model performance. However, the UAR1 model is still the best performing alternative compare to the relative wetness index and temporal stability disaggregation methods in this catchment (not shown).

The ranges of spatial correlations between soil moisture distributions for every simulation year are higher for scenarios 1 and 5 and are lower for the steep and randomly heterogeneous soil texture indicator field. The percentage of times in a simulation year where NSE is larger than 0 is larger in 2008 and 2010 relative to the 2006 dry year and is close to 100% for scenario 4. While the UAR1.c model results in the same catchment-averaged soil moisture as the fully distributed SMART simulation, because of the similarity of catchment mean soil moisture between the three ECSs and the fully distributed case, the spatial standard deviation of disaggregated soil moisture fields is higher than the SMART reference case. This results in zero or negative NSE values in some time steps as shown in Figure 16.

NSE value of disaggregated soil moisture time series at every pixel against the SMART fully distributed simulations for each scenario is quite high and is close to 1 in most cases (see Figure 17). These results highlight that despite the degradation of spatial NSE, the temporal dynamics of soil moisture for every pixel in the domain is captured well by the UAR1.c model except for scenario 3 (indicator random field) (Figure 17).

Results of the sensitivity analysis to changes in catchment characteristics illustrate that sensitivity to soil texture heterogeneity is higher than topography in a set of scenarios explored here. However, not all types of subsurface heterogeneity results in larger spatial disaggregation errors, and the magnitude of errors depends on the soil-type heterogeneity patterns. Despite decreases in spatial NSE for different scenarios, UAR1.c model still performs better than other alternatives for scenarios explored here particularly with respect to preserving temporal persistence. This result suggests that the UAR1 model has the potential for disaggregating catchment mean soil moisture from satellite observations or semidistributed model simulations.

## 5. Conclusions

We developed a hybrid statistical approach based on the UAR1 model to disaggregate catchment mean soil moisture to fine-resolution soil moisture distribution. Results of validation periods show that the autoregressive models and temporal stability methods perform very well with daily NSE values of greater than 0.7 and 0.3, respectively, when data from the entire domain are used for model parameterization. The lower NSE values during 2010 validation year are related to increases in water table elevation during intense rainfall events that is not accounted for in formulating the statistical models. Overall, the AR1 model predictions are superior to the temporal stability method during 2010 period. Using soil moisture simulations across a

series of distributed cross sections to parameterize the statistical models deteriorates model performance at the interpolated pixels. Nevertheless, the UAR1 model performs best compared to the disaggregation methods based on the relative wetness index, TOPMODEL, or temporal stability methods particularly when spatial standard deviation of soil moisture predictions from the AR1 models are updated based on the catchment mean soil moisture. However, reliance on fine-scale model simulations for constructing the **A** matrix as well as reliance on unbiased catchment mean soil moisture from satellite observations or coarse model simulations remains a challenge.

Sensitivity analysis results illustrate that only 10 days of fine-resolution soil moisture simulations preferably from a drier period is required for calibrating the statistical models using simulations from the entire domain or cross sections. Sensitivity analysis results to changes in catchment characteristics illustrate that subsurface heterogeneity has larger impact than the topography in a set of scenarios explored here, and the magnitude of errors depends on soil-type heterogeneity patterns. Nevertheless, the UAR1 model preserves pixel-based temporal variability of disaggregated soil moisture better than other alternatives in our scenarios. The advantage of the cross-section approach is in its computational efficiency, and it has the potential for soil moisture spatial disaggregation in semidistributed modeling frameworks. These fine-resolution soil moisture estimations are important for evapotranspiration and runoff estimation, irrigation management, and characterizing land-atmosphere feedbacks (Pau et al., 2016).

**Acknowledgments**
This research was funded by the Australian Research Council and USDA multi-state W3188 project. We acknowledge the support provided by the National Computational Infrastructure at the Australian National University through the Intersect partner share for high-performance computing. We would like to thank the New South Wales Department of Primary Industries for providing Baldry meteorological data and Julian Koch for providing the EOF analysis code. Data and model codes are available through UCR Dash, research data repository of University of California Riverside (https://doi.org/10.6086/D1B955).

## References

Acworth, R. I., & Brain, T. (2008). Calculation of barometric efficiency in shallow piezometers using water levels, atmospheric and Earth tide data. *Hydrogeology Journal*, *16*(8), 1469–1481. https://doi.org/10.1007/s10040-008-0333-y

Ajami, H., Evans, J. P., McCabe, M. F., & Stisen, S. (2014). Technical note: Reducing the spin-up time of integrated surface water–groundwater models. *Hydrology and Earth System Sciences*, *18*(12), 5169–5179. https://doi.org/10.5194/hess-18-5169-2014

Ajami, H., Khan, U., Tuteja, N. K., & Sharma, A. (2016). Development of a computationally efficient semi-distributed hydrologic modeling application for soil moisture, lateral flow and runoff simulation. *Environmental Modelling & Software*, *85*, 319–331. https://doi.org/10.1016/j.envsoft.2016.09.002

Ashby, S. F., & Falgout, R. D. (1996). A parallel multigrid preconditioned conjugate gradient algorithm for groundwater flow simulations. *Nuclear Science and Engineering*, *124*(1), 145–159. https://doi.org/10.13182/NSE96-A24230

Best, M. J., Abramowitz, G., Johnson, H. R., Pitman, A. J., Balsamo, G., Boone, A., et al. (2015). The plumbing of land surface models: Benchmarking model performance. *Journal of Hydrometeorology*, *16*(3), 1425–1442. https://doi.org/10.1175/JHM-D-14-0158.1

Beven, K. (1997). TOPMODEL: A critique. *Hydrological Processes*, *11*(9), 1069–1085. https://doi.org/10.1002/(SICI)1099-1085(199707)11:9<1069::AID-HYP545>3.0.CO;2-O

Beven, K. J., & Kirkby, M. J. (1979). A physically based, variable contributing area model of basin hydrology. *Hydrological Sciences Bulletin*. https://doi.org/10.1080/02626667909491834

Chan, S. K., Bindlish, R., O'Neill, P., Jackson, T., Njoku, E., Dunbar, S., et al. (2018). Development and assessment of the SMAP enhanced passive soil moisture product. *Remote Sensing of Environment*, *204*, 931–941. https://doi.org/10.1016/j.rse.2017.08.025

Chaney, N. W., Metcalfe, P., & Wood, E. F. (2016). HydroBlocks: A field-scale resolving land surface model for application over continental extents. *Hydrological Processes*, *30*(20), 3543–3559. https://doi.org/10.1002/hyp.10891

Choi, H. I., Kumar, P., & Liang, X.-Z. (2007). Three-dimensional volume-averaged soil moisture transport model with a scalable parameterization of subgrid topographic variability. *Water Resources Research*, *43*, W04414. https://doi.org/10.1029/2006WR005134

Dai, Y., Zeng, X., Dickinson, R. E., Baker, I., Bonan, G. B., Bosilovich, M. G., et al. (2003). The common land model. *Bulletin of the American Meteorological Society*, *84*(8), 1013–1024. https://doi.org/10.1175/bams-84-8-1013

Decker, M., Pitman, A. J., & Evans, J. P. (2012). Groundwater constraints on simulated transpiration variability over southeastern Australian forests. *Journal of Hydrometeorology*, *14*(2), 543–559. https://doi.org/10.1175/JHM-D-12-058.1

Delworth, T. L., & Manabe, S. (1988). The influence of potential evaporation on the variabilities of simulated soil wetness and climate. *Journal of Climate*, *1*(5), 523–547. https://doi.org/10.1175/1520-0442(1988)001<0523:TIOPEO>2.0.CO;2

Entin, J. K., Robock, A., Vinnikov, K. Y., Hollinger, S. E., Liu, S., & Namkhai, A. (2000). Temporal and spatial scales of observed soil moisture variations in the extratropics. *Journal of Geophysical Research*, *105*(D9), 11,865–11,877. https://doi.org/10.1029/2000JD900051

Famiglietti, J. S., Devereaux, J. A., Laymon, C. A., Tsegaye, T., Houser, P. R., Jackson, T. J., et al. (1999). Ground-based investigation of soil moisture variability within remote sensing footprints during the Southern Great Plains 1997 (SGP97) hydrology experiment. *Water Resources Research*, *35*(6), 1839–1851. https://doi.org/10.1029/1999WR900047

Famiglietti, J. S., Ryu, D., Berg, A. A., Rodell, M., & Jackson, T. J. (2008). Field observations of soil moisture variability across scales. *Water Resources Research*, *44*, W01423. https://doi.org/10.1029/2006WR005804

Fatichi, S., Vivoni, E. R., Ogden, F. L., Ivanov, V. Y., Mirus, B., Gochis, D., et al. (2016). An overview of current applications, challenges, and future trends in distributed process-based models in hydrology. *Journal of Hydrology*, *537*, 45–60. https://doi.org/10.1016/j.jhydrol.2016.03.026

Gaur, N., & Mohanty, B. P. (2013). Evolution of physical controls for soil moisture in humid and subhumid watersheds. *Water Resources Research*, *49*, 1244–1258. https://doi.org/10.1002/wrcr.20069

Ghannam, K., Nakai, T., Paschalis, A., Oishi, C. A., Kotani, A., Igarashi, Y., et al. (2016). Persistence and memory timescales in root-zone soil moisture dynamics. *Water Resources Research*, *52*, 1427–1445. https://doi.org/10.1002/2015WR017983

Grayson, R., & Western, A. (2001). Terrain and the distribution of soil moisture. *Hydrological Processes*, *15*(13), 2689–2690. https://doi.org/10.1002/hyp.479

Grayson, R. B., Western, A. W., Chiew, F. H. S., & Blöschl, G. (1997). Preferred states in spatial soil moisture patterns: Local and nonlocal controls. *Water Resources Research*, *33*(12), 2897–2908. https://doi.org/10.1029/97WR02174

Gupta, H. V., Kling, H., Yilmaz, K. K., & Martinez, G. F. (2009). Decomposition of the mean squared error and NSE performance criteria: Implications for improving hydrological modelling. *Journal of Hydrology*, *377*(1-2), 80–91. https://doi.org/10.1016/j.jhydrol.2009.08.003

Jana, R. B., & Mohanty, B. P. (2012a). A comparative study of multiple approaches to soil hydraulic parameter scaling applied at the hillslope scale. *Water Resources Research*, *48*, W02520. https://doi.org/10.1029/2010WR010185

Jana, R. B., & Mohanty, B. P. (2012b). On topographic controls of soil hydraulic parameter scaling at hillslope scales. *Water Resources Research*, *48*, W02518. https://doi.org/10.1029/2011WR011204

Jawson, S. D., & Niemann, J. D. (2007). Spatial patterns from EOF analysis of soil moisture at a large scale and their dependence on soil, land-use, and topographic properties. *Advances in Water Resources*, *30*(3), 366–381. https://doi.org/10.1016/j.advwatres.2006.05.006

Jones, J. E., & Woodward, C. S. (2001). Newton–Krylov-multigrid solvers for large-scale, highly heterogeneous, variably saturated flow problems. *Advances in Water Resources*, *24*(7), 763–774. https://doi.org/10.1016/s0309-1708(00)00075-0

Joshi, C., Mohanty, B. P., Jacobs, J. M., & Ines, A. V. M. (2011). Spatiotemporal analyses of soil moisture from point to footprint scale in two different hydroclimatic regions. *Water Resources Research*, *47*, W01508. https://doi.org/10.1029/2009WR009002

Khan, U., Ajami, H., Tuteja, N. K., Sharma, A., & Kim, S. (2018). Catchment scale simulations of soil moisture dynamics using an equivalent cross-section based hydrological modelling approach. *Journal of Hydrology*, *564*, 944–966. https://doi.org/10.1016/j.jhydrol.2018.07.066

Khan, U., Tuteja, N. K., Ajami, H., & Sharma, A. (2014). An equivalent cross-sectional basis for semidistributed hydrological modeling. *Water Resources Research*, *50*, 4395–4415. https://doi.org/10.1002/2013WR014741

Khan, U., Tuteja, N. K., & Sharma, A. (2013). Delineating hydrologic response units in large upland catchments and its evaluation using soil moisture simulations. *Environmental Modelling & Software*, *46*, 142–154. https://doi.org/10.1016/j.envsoft.2013.03.005

Kim, J., Dwelle, M. C., Kampf, S. K., Fatichi, S., & Ivanov, V. Y. (2016). On the non-uniqueness of the hydro-geomorphic responses in a zero-order catchment with respect to soil moisture. *Advances in Water Resources*, *92*, 73–89. https://doi.org/10.1016/j.advwatres.2016.03.019

Kim, S., Balakrishnan, K., Liu, Y., Johnson, F., & Sharma, A. (2017). Spatial disaggregation of coarse soil moisture data by using high-resolution remotely sensed vegetation products. *IEEE Geoscience and Remote Sensing Letters*, *14*(9), 1604–1608. https://doi.org/10.1109/LGRS.2017.2725945

Koch, J., Jensen, K. H., & Stisen, S. (2015). Toward a true spatial model evaluation in distributed hydrological modeling: Kappa statistics, fuzzy theory, and EOF analysis benchmarked by the human perception and evaluated against a modeling case study. *Water Resources Research*, *51*, 1225–1246. https://doi.org/10.1002/2014WR016607

Koch, J., Mendiguren, G., Mariethoz, G., & Stisen, S. (2017). Spatial sensitivity analysis of simulated land surface patterns in a catchment model using a set of innovative spatial performance metrics. *Journal of Hydrometeorology*, *18*(4), 1121–1142. https://doi.org/10.1175/JHM-D-16-0148.1

Kollet, S. J., & Maxwell, R. M. (2006). Integrated surface–groundwater flow modeling: A free-surface overland flow boundary condition in a parallel groundwater flow model. *Advances in Water Resources*, *29*(7), 945–958. https://doi.org/10.1016/j.advwatres.2005.08.006

Kollet, S. J., & Maxwell, R. M. (2008). Capturing the influence of groundwater dynamics on land surface processes using an integrated, distributed watershed model. *Water Resources Research*, *44*, W02402. https://doi.org/10.1029/2007WR006004

Korres, W., Reichenau, T. G., Fiener, P., Koyama, C. N., Bogena, H. R., Cornelissen, T., et al. (2015). Spatio-temporal soil moisture patterns—A meta-analysis using plot to catchment scale data. *Journal of Hydrology*, *520*, 326–341. https://doi.org/10.1016/j.jhydrol.2014.11.042

Koster, R. D., Suarez, M. J., Ducharne, A., Stieglitz, M., & Kumar, P. (2000). A catchment-based approach to modeling land surface processes in a general circulation model: 1. Model structure. *Journal of Geophysical Research*, *105*(D20), 24,809–24,822. https://doi.org/10.1029/2000JD900327

Loew, A., & Mauser, W. (2008). On the disaggregation of passive microwave soil moisture data using a priori knowledge of temporally persistent soil moisture fields. *IEEE Transactions on Geoscience and Remote Sensing*, *46*(3), 819–834. https://doi.org/10.1109/TGRS.2007.914800

Mascaro, G., Vivoni, E. R., & Méndez-Barroso, L. A. (2015). Hyperresolution hydrologic modeling in a regional watershed and its interpretation using empirical orthogonal functions. *Advances in Water Resources*, *83*, 190–206. https://doi.org/10.1016/j.advwatres.2015.05.023

Matalas, N. C. (1967). Mathematical assessment of synthetic hydrology. *Water Resources Research*, *3*(4), 937–945. https://doi.org/10.1029/WR003i004p00937

Mauser, W., & Schädlich, S. (1998). Modelling the spatial distribution of evapotranspiration on different scales using remote sensing data. *Journal of Hydrology*, *212–213*, 250–267. https://doi.org/10.1016/S0022-1694(98)00228-5

Maxwell, R. M., & Miller, N. L. (2005). Development of a coupled land surface and groundwater model. *Journal of Hydrometeorology*, *6*(3), 233–247. https://doi.org/10.1175/JHM422.1

Mehrotra, R., & Sharma, A. (2015). Correcting for systematic biases in multiple raw GCM variables across a range of timescales. *Journal of Hydrology*, *520*, 214–223. https://doi.org/10.1016/j.jhydrol.2014.11.037

Merlin, O., Escorihuela, M. J., Mayoral, M. A., Hagolle, O., Al Bitar, A., & Kerr, Y. (2013). Self-calibrated evaporation-based disaggregation of SMOS soil moisture: An evaluation study at 3 km and 100 m resolution in Catalunya, Spain. *Remote Sensing of Environment*, *130*, 25–38. https://doi.org/10.1016/j.rse.2012.11.008

Merlin, O., Walker, J. P., Chehbouni, A., & Kerr, Y. (2008). Towards deterministic downscaling of SMOS soil moisture using MODIS derived soil evaporative efficiency. *Remote Sensing of Environment*, *112*(10), 3935–3946. https://doi.org/10.1016/j.rse.2008.06.012

Mohanty, B. P., Cosh, M. H., Lakshmi, V., & Montzka, C. (2017). Soil moisture remote sensing: State-of-the-science. *Vadose Zone Journal*, *16*(1). https://doi.org/10.2136/vzj2016.10.0105

Pau, G. S. H., Shen, C., Riley, W. J., & Liu, Y. (2016). Accurate and efficient prediction of fine-resolution hydrologic and carbon dynamic simulations from coarse-resolution models. *Water Resources Research*, *52*, 791–812. https://doi.org/10.1002/2015WR017782

Peel, M. C., Finlayson, B. L., & McMahon, T. A. (2007). Updated world map of the Köppen-Geiger climate classification. *Hydrology and Earth System Sciences*, *11*(5), 1633–1644. https://doi.org/10.5194/hess-11-1633-2007

Pellenq, J., Kalma, J., Boulet, G., Saulnier, G. M., Wooldridge, S., Kerr, Y., & Chehbouni, A. (2003). A disaggregation scheme for soil moisture based on topography and soil depth. *Journal of Hydrology*, *276*(1–4), 112–127. https://doi.org/10.1016/S0022-1694(03)00066-0

Peng, J., Loew, A., Merlin, O., & Verhoest, N. E. C. (2017). A review of spatial downscaling of satellite remotely sensed soil moisture. *Reviews of Geophysics*, *55*, 341–366. https://doi.org/10.1002/2016RG000543

Perry, M. A., & Niemann, J. D. (2007). Analysis and estimation of soil moisture at the catchment scale using EOFs. *Journal of Hydrology*, *334*(3–4), 388–404. https://doi.org/10.1016/j.jhydrol.2006.10.014

Quinn, P. F., Beven, K. J., & Lamb, R. (1995). The in(a/tan/β) index: How to calculate it and how to use it within the topmodel framework. *Hydrological Processes*, *9*(2), 161–182. https://doi.org/10.1002/hyp.3360090204

Reynolds, S. G. (1970). The gravimetric method of soil moisture determination. Part III: An examination of factors influencing soil moisture variability. *Journal of Hydrology*, *11*(3), 288–300. https://doi.org/10.1016/0022-1694(70)90068-5

Richards, L. A. (1931). Capillary conduction of liquids in porous mediums. *Journal of Applied Physics*, *1*(5), 318–333. https://doi.org/10.1063/1.1745010

Riley, W. J., & Shen, C. (2014). Characterizing coarse-resolution watershed soil moisture heterogeneity using fine-scale simulations. *Hydrology and Earth System Sciences*, *18*(7), 2463–2483. https://doi.org/10.5194/hess-18-2463-2014

Rodriguez-Iturbe, I., Vogel, G. K., Rigon, R., Entekhabi, D., Castelli, F., & Rinaldo, A. (1995). On the spatial organization of soil moisture fields. *Geophysical Research Letters*, *22*(20), 2757–2760. https://doi.org/10.1029/95GL02779

Rosenbaum, U., Bogena, H. R., Herbst, M., Huisman, J. A., Peterson, T. J., Weuthen, A., et al. (2012). Seasonal and event dynamics of spatial soil moisture patterns at the small catchment scale. *Water Resources Research*, *48*, W10544. https://doi.org/10.1029/2011WR011518

Salas, J. D., Deulleur, J. W., Yevjevich, V., & Lane, W. L. (1980). *Applied modelling of hydrologic time series*. Littleton, Colorado, USA: Water Resources Publ.

Salas, J. D., Tabios, G. Q., & Bartolini, P. (1985). Approaches to multivariate modeling of water resources time series. *JAWRA Journal of the American Water Resources Association*, *21*(4), 683–708. https://doi.org/10.1111/j.1752-1688.1985.tb05383.x

Seneviratne, S. I., Corti, T., Davin, E. L., Hirschi, M., Jaeger, E. B., Lehner, I., et al. (2010). Investigating soil moisture-climate interactions in a changing climate: A review. *Earth-Science Reviews*, *99*(3–4), 125–161. https://doi.org/10.1016/j.earscirev.2010.02.004

Shin, Y., & Mohanty, B. P. (2013). Development of a deterministic downscaling algorithm for remote sensing soil moisture footprint using soil and vegetation classifications. *Water Resources Research*, *49*, 6208–6228. https://doi.org/10.1002/wrcr.20495

Tuteja, N.K., Vaze, J., Murphy, B., & Beale, G. T. B. (2004). CLASS: catchment scale multiple-landuse atmosphere soil water and solute transport model. Retrieved from https://toolkit.ewater.org.au/Tools/CLASS-U3M-1D

Vachaud, G., Passerat De Silans, A., Balabanis, P., & Vauclin, M. (1985). Temporal stability of spatially measured soil water probability density function. *Soil Science Society of America Journal*, *49*(4), 822–828. https://doi.org/10.2136/sssaj1985.03615995004900040006x

Vanderlinden, K., Vereecken, H., Hardelauf, H., Herbst, M., Martínez, G., Cosh, M. H., & Pachepsky, Y. A. (2012). Temporal stability of soil water contents: A review of data and analyses. *Vadose Zone Journal*, *11*(4). https://doi.org/10.2136/vzj2011.0178

Vereecken, H., Huisman, J. A., Pachepsky, Y., Montzka, C., van der Kruk, J., Bogena, H., Weihermüller, L., et al. (2012). On the spatio-temporal dynamics of soil moisture at the field scale. *Journal of Hydrology*, *516*, 76–96. https://doi.org/10.1016/j.jhydrol.2013.11.061

Western, A. W., Zhou, S.-L., Grayson, R. B., McMahon, T. A., Blöschl, G., & Wilson, D. J. (2004). Spatial correlation of soil moisture in small catchments and its relationship to dominant spatial hydrological processes. *Journal of Hydrology*, *286*(1–4), 113–134, 134. https://doi.org/10.1016/j.jhydrol.2003.09.014

Westra, S., Brown, C., Lall, U., & Sharma, A. (2007). Modeling multivariable hydrological series: Principal component analysis or independent component analysis? *Water Resources Research*, *43*, W06429. https://doi.org/10.1029/2006WR005617

Wilson, D. J., Western, A. W., & Grayson, R. B. (2005). A terrain and data-based method for generating the spatial distribution of soil moisture. *Advances in Water Resources*, *28*(1), 43–54. https://doi.org/10.1016/j.advwatres.2004.09.007

Wood, E. F., Roundy, J. K., Troy, T. J., van Beek, L. P. H., Bierkens, M. F. P., Blyth, E., et al. (2011). Hyperresolution global land surface modeling: Meeting a grand challenge for monitoring Earth's terrestrial water. *Water Resources Research*, *47*, W05301. https://doi.org/10.1029/2010WR010090